

AD-A089 649

R AND D ASSOCIATES MARINA DEL REY CA

F/O 20/14

ELECTROMAGNETIC SCATTERING BY AN OBJECT EMBEDDED IN A STRATIFIED MEDIUM

AUG 80 M I SANCER, S SIEGEL, D S GOODROW

F29601-78-C-0096

UNCLASSIFIED

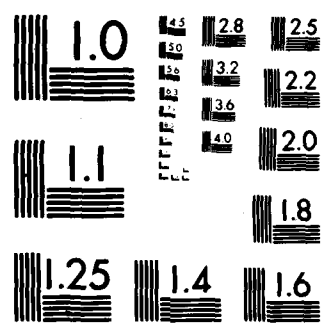
RDA-TR-110400-002

AFWL-TR-80-30

NL

1 of 1
AD-A089 649

END
DATE
FILMED
10-80
DTIC



MICROCOPY RESOLUTION TEST CHART
NATIONAL BUREAU OF STANDARDS-1963-A

AFWL-TR-80-30

② **LEVEL III**
B.S.

AD-E 200 557

AFWL-TR
80-30

AD A089649

ELECTROMAGNETIC SCATTERING BY AN OBJECT EMBEDDED IN A STRATIFIED MEDIUM

M. I. Sancer
S. Siegel
D. S. Goodrow

R&D Associates
Marina del Rey, CA 90291

August 1980

Final Report

Approved for public release; distribution unlimited.

DTIC
ELECTE
SEP 26 1980
S B D

AIR FORCE WEAPONS LABORATORY
Air Force Systems Command
Kirtland Air Force Base, NM 87117

DC FILE COPY


This final report was prepared by the R & D Associates, Marina del Rey, California, under Contract F29601-78-C-0098, Job Order 37630134 with the Air Force Weapons Laboratory, Kirtland Air Force Base, New Mexico. Captain Howard G. Hudson (NTY) was the Laboratory Project Officer-in-Charge.

When US Government drawings, specifications, or other data are used for any purpose other than a definitely related Government procurement operation, the Government thereby incurs no responsibility nor any obligation whatsoever, and the fact that the Government may have formulated, furnished, or in any way supplied the said drawings, specifications, or other data, is not to be regarded by implication or otherwise, as in any manner licensing the holder or any other person or corporation, or conveying any rights or permission to manufacture, use, or sell any patented invention that may in any way be related thereto.

This report has been authored by a contractor of the United States Government. Accordingly, the United States Government retains a nonexclusive, royalty-free license to publish or reproduce the material contained herein, or allow others to do so, for the United States Government purposes.

This report has been reviewed by the Public Affairs Office and is releasable to the National Technical Information Service (NTIS). At NTIS, it will be available to the general public, including foreign nations.

This technical report has been reviewed and is approved for publication.



HOWARD G. HUDSON
Captain, USAF
Project Officer



PHILIP CASTILLO
Chief, Electromagnetics Branch

FOR THE DIRECTOR



THOMAS W. CIAMBRONE
Colonel, USAF
Chief, Applied Physics Division

DO NOT RETURN THIS COPY. RETAIN OR DESTROY.

UNCLASSIFIED

SECURITY CLASSIFICATION OF THIS PAGE (When Data Entered)

REPORT DOCUMENTATION PAGE		READ INSTRUCTIONS BEFORE COMPLETING FORM
1. REPORT NUMBER AFWL-TR-80-30	2. GOVT ACCESSION NO. AD-A089649	3. RECIPIENT'S CATALOG NUMBER
4. TITLE (and Subtitle) ELECTROMAGNETIC SCATTERING BY AN OBJECT EMBEDDED IN A STRATIFIED MEDIUM		5. TYPE OF REPORT & PERIOD COVERED Final Report
7. AUTHOR(s) Maurice I. Sancer Scott Siegel Dennis S. Goodrow		6. PERFORMING ORG. REPORT NUMBER RDA-TR-110400-002 ✓
9. PERFORMING ORGANIZATION NAME AND ADDRESS R&D Associates P. O. Box 9695 Marina del Rey, CA 90291		8. CONTRACT OR GRANT NUMBER(s) F29601-78-C-0098 <i>nmw</i>
11. CONTROLLING OFFICE NAME AND ADDRESS Air Force Weapons Laboratory (NTY) Kirtland Air Force Base, NM 87117		10. PROGRAM ELEMENT, PROJECT, TASK AREA & WORK UNIT NUMBERS 64711F/37630134
14. MONITORING AGENCY NAME & ADDRESS (if different from Controlling Office)		12. REPORT DATE August 1980
		13. NUMBER OF PAGES 92
		15. SECURITY CLASS. (of this report) Unclassified
		15a. DECLASSIFICATION/DOWNGRADING SCHEDULE
16. DISTRIBUTION STATEMENT (of this Report) Approved for public release; distribution unlimited.		
17. DISTRIBUTION STATEMENT (of the abstract entered in Block 20, if different from Report)		
18. SUPPLEMENTARY NOTES		
19. KEY WORDS (Continue on reverse side if necessary and identify by block number) Aircraft Model Lossy Earth Interaction Computer Code		
20. ABSTRACT (Continue on reverse side if necessary and identify by block number) A general electromagnetic scattering formulation is presented for the situation in which a perfectly conducting body is embedded in a horizontally or radially stratified medium. The electric field integro-differential equation (EFIDE) and magnetic field integral equation (MFIE) are derived for the determination of the surface current density induced on the body by a general class of sources. Expressions are also presented for the use of the current density to determine the electric and magnetic fields scattered by the body into any layer of the medium. (over)		

DD FORM 1 JAN 73 1473

UNCLASSIFIED

SECURITY CLASSIFICATION OF THIS PAGE (When Data Entered)

UNCLASSIFIED

SECURITY CLASSIFICATION OF THIS PAGE(When Data Entered)

20. ABSTRACT

Detailed expressions for the MFIE and EFIDE are presented for the horizontally stratified two-layered medium configuration corresponding to the object being in a vacuum half-space above a lossy half-space. A computer code, which is an extended version of NEC-2A, is developed for the solution of the two-layer MFIE for a situation where the object is a model of an aircraft. Results corresponding to special cases obtained by this computer code are compared to experimental data as well as to numerical results obtained by another independently developed computer code.

ACCESSION for	
NTIS	White Section <input checked="" type="checkbox"/>
DDC	Buff Section <input type="checkbox"/>
UNANNOUNCED	<input type="checkbox"/>
JUSTIFICATION	
BY	
DISTRIBUTION/AVAILABILITY CODES	
Dist. AVAIL. and/or SPECIAL	
A	-

UNCLASSIFIED

SECURITY CLASSIFICATION OF THIS PAGE(When Data Entered)

TABLE OF CONTENTS

<u>Section</u>		<u>Page</u>
I	INTRODUCTION	7
II	SURFACE INTEGRAL REPRESENTATIONS FOR SCATTERING BY AN OBJECT EMBEDDED IN A STRATIFIED MEDIUM	11
III	EXPLICIT GREEN'S DYADIC REPRESENTATIONS FOR THE TWO-LAYERED CONFIGURATION OF INTEREST	22
IV	EXPLICIT REPRESENTATIONS FOR $\underline{E}_T(\underline{r})$ AND $\underline{H}_T(\underline{r})$ FOR THE TWO-LAYERED PROBLEM OF INTEREST	34
V	PRESENTATION OF THE MAGNETIC FIELD INTEGRAL EQUATION (MFIE) AND THE ELECTRIC FIELD INTEGRO-DIFFERENTIAL EQUATION (EFIDE) FOR THE STRATIFIED MEDIUM SCATTERING PROBLEM	39
VI	EXPLICIT SYMMETRY ARGUMENTS FOR THE TWO-LAYERED MFIE	48
VII	CODE TESTING	62
	1. Introduction	62
	2. Verification of Basic Quantities	65
	3. Usage of the Lossy Half-Space Terms	67
	4. Free Space Limit	68
	5. Comparison to Another Code	69
	6. Comparison to Experimental Data	69
	7. Accuracy Considerations	78

TABLE OF CONTENTS (CONCLUDED)

<u>Section</u>	<u>Page</u>
REFERENCES	81
APPENDIX A. PROOF THAT $F_{N_{sab}}$ IS INDEPENDENT OF THE SCATTERING OBJECT	83
APPENDIX B. PROOF THAT $\underline{G}_j(\underline{r}, \underline{r}') = \underline{G}_k(\underline{r}', \underline{r})$	87
APPENDIX C. OUTLINE OF ESSENTIAL DETAILS TO DERIVE EQUATION 38	90

LIST OF FIGURES

<u>Figure</u>		<u>Page</u>
1	Aircraft Model	8
2a	Horizontally Stratified Medium Configuration	12
2b	Radially Stratified Medium Configuration	12
3	Coordinate Systems	24
4	Description of the Incident Plane Electromagnetic Wave. Axis x is the Intersection of the z,k Plane and a Plane Perpendicular to k at the Origin	63
5	Comparison Between "Free Cylinder" Experimental Results at University of Michigan (Solid Curves) and MFIE Computer Code (Dots)	71
6	Comparison Between "Cylinder Parallel to a Perfectly Conducting Ground" Experimental Results at University of Michigan (Solid Curve) and MFIE Computer Code (Dots) for $d = 5a$	72
7	Comparison Between "Cylinder Parallel to Perfectly Conducting Ground" Experimental Results at University of Michigan (Solid Curve) and MFIE Computer Code (Dots) for $d = 1.5a$	73
8	Comparison Between the MFIE Computer Code (Dots) and the "Cylinder Parallel to a Finitely Conducting Ground" Experimental Results at University of Michigan (Solid Curve) for $d = 5a$	75
9	Comparison Between the MFIE Computer Code (Dots) and the "Cylinder Parallel to a Finitely Conducting Ground" Experimental Results at University of Michigan (Solid Curve) for $d = 2a$	76

LIST OF FIGURES (CONCLUDED)

<u>Figure</u>		<u>Page</u>
10	Comparison Between the MFIE Computer Code (Dots) and the "Cylinder Parallel to a Finitely Conducting Ground" Experimental Results at University of Michigan (Solid Curve) for $d = 1.5a$	77

LIST OF TABLES

<u>Table</u>		<u>Page</u>
1	Configuration Parameters for Comparison to the Lawrence Livermore Laboratory's Nuclear Electromagnetics Code (L ³ NEC)	70
2	Predicted Bulk Currents	70
3	Complex Dielectric Constant used in the MFIE Computer Code Calculations Applicable for the University of Michigan Experimental Data	74

I. INTRODUCTION

In Reference 1 we presented a derivation of both the electric field integro-differential equation (EFIDE) and the magnetic field integral equation (MFIE) for the determination of the current density induced on the surface of metallic (perfectly conducting) structures situated in a vacuum half-space above a lossy half-space. We showed, by comparison to experiments performed at the University of Michigan, the quality of the predictions that could be obtained by using the patch zoning method to solve the MFIE for two limiting cases of the lossy half-space: free-space and perfectly conducting. The code developed for this purpose is capable of obtaining surface current predictions for an aircraft model consisting of intersecting elliptical cylinders (Figure 1), optionally in the presence of a perfectly conducting ground plane. Reference 1 presents comparisons of predictions versus experiments for the full aircraft model situated in free-space as well as a cylinder above a perfectly conducting half-space.

In this report we present the result of our efforts to enhance our computer code (NEC-2A) by including the capability to treat the same aircraft model in the presence of a lossy half-space. Before embarking on the extensive programming effort required to solve the MFIE for the two-layered problem, we checked the validity of our equations by rederiving them in an alternate manner. We present this derivation here, as well as its generalization to multilayered horizontally or radially stratified media. We show that the electric dipole-excited electric or magnetic fields are the fundamental quantities required to determine the EFIDE and the MFIE respectively. We utilize these dipole-excited quantities to construct Green's dyadics, and the procedure for doing this is presented in detail. The determination of these dipole-excited fields is basically as

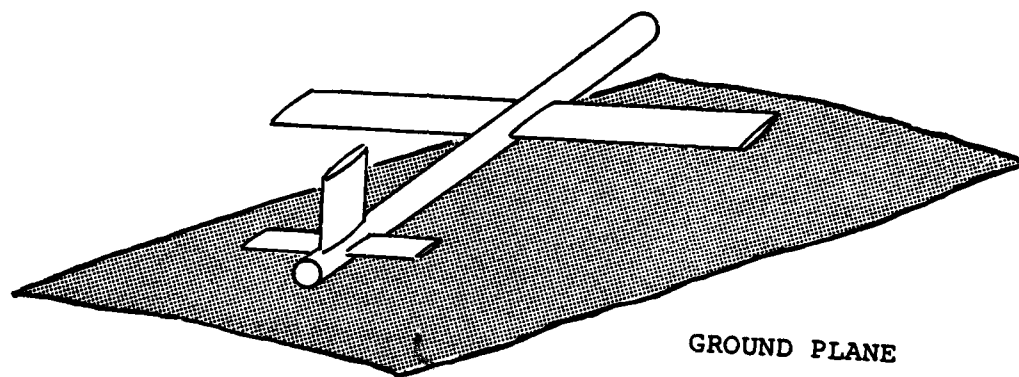


Figure 1. Aircraft Model

tractable for the multilayered problem as it is for the two-layered problem. Following a procedure presented in the book by Felsen and Marcuvitz (Reference 2), one can determine all the necessary dipole-excited fields from scalar potentials. Utilizing these potentials and satisfying boundary conditions leads to a system of linear algebraic equations for a finite number of unknown constants and this number depends linearly on the number of layers used to describe the medium. If we intend to develop a computer code for the use of the dipole solutions, e.g., the MFIE, then the code can be written to solve the finite system of equations as part of its execution. To make the existence of the dipole-excited solutions have more than just a potential role for future work, we present the explicit use of these dipole solutions (Reference 3) for the horizontally stratified two-layered medium to obtain exactly the same EFIE and MFIE derived in Reference 1 and thus complete the desired alternate derivation. Further use of our general formulation can be made by using both the analysis and computer code described in Reference 4 for the horizontally stratified three-layered medium. Additional material on dipole-excited fields in a multilayered medium can be found in Reference 5.

We exercised certain switches in the computer code developed for the two-layered problem to compare our code's capabilities to two other sets of data for the response of a perfectly conducting, finite length cylinder in the proximity of planar lossy material. One set of data is the current density measured on the cylinder when it was placed in front of lossy material within the anechoic chamber at the University of Michigan (Reference 6). The other set of data furnished to us by G. J. Burke was calculated as a special case of a Lawrence Livermore Laboratory code's capability which corresponds to a special case of our code's capability. A more detailed description of that code can be found in Reference 7. This data was the plane

wave induced bulk current on a finite cylinder above and parallel to a lossy half-space. The results of both the Michigan and Livermore comparisons as well as other intermediate tests are presented in this report.

II. SURFACE INTEGRAL REPRESENTATIONS FOR SCATTERING BY AN OBJECT EMBEDDED IN A STRATIFIED MEDIUM

The presentation of this analysis is facilitated by referring to Figure 2. In that figure we divide all of space into N distinct volumes and label the volume containing the object with the index N_s . Each volume is characterized by different electrical parameters so that Maxwell's equations appropriate for a particular volume V_ℓ are written as

$$\nabla \times \underline{E}_{\ell\alpha}(\underline{r}) = i\omega\mu_\ell \underline{H}_{\ell\alpha}(\underline{r}) \quad (1)$$

$$\nabla \times \underline{H}_{\ell\alpha}(\underline{r}) = -i\omega\epsilon_\ell \underline{E}_{\ell\alpha}(\underline{r}) + \underline{J}_{\ell\alpha}(\underline{r}) \quad (2)$$

where $\ell=1,2,\dots,N$ and for the case that will be developed in most detail

$$\epsilon_\ell = \epsilon_{\ell R} + i\epsilon_{\ell I} \quad (3)$$

The rigid source terms satisfy the condition

$$\underline{J}_{\ell\alpha}(\underline{r}) \neq 0 \text{ only if } \underline{r} \in V_{\ell\alpha} \subset V_\ell \quad (4)$$

and in this section $\alpha=a$ will correspond to mathematically introduced delta function sources and $\alpha=b$ will correspond to the physical distribution of sources. The analysis that will be presented has applicability for more general situations than the stratified model of all space depicted in Figure 2; however, that situation includes all cases of current interest.

When the sources are delta function sources located at a point \underline{r}_α , then we introduce the common notation

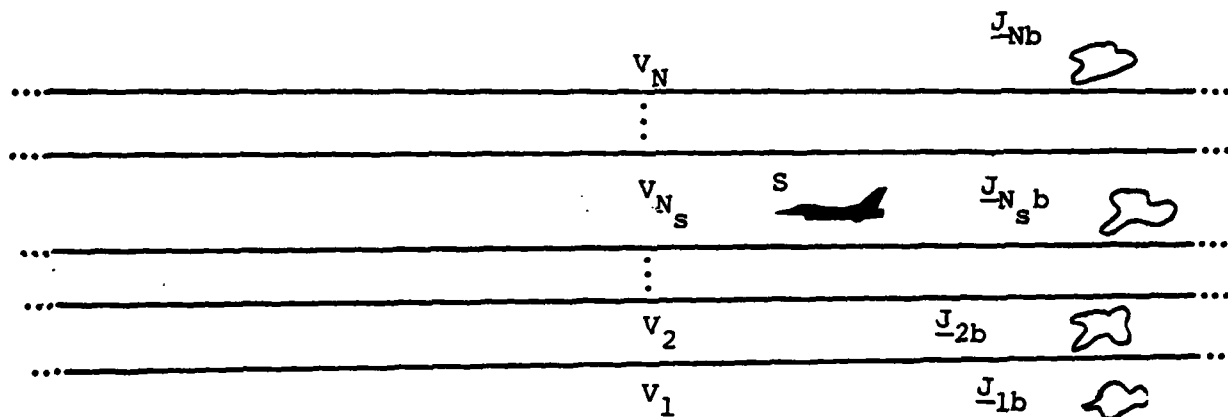


Figure 2a. Horizontally stratified medium configuration

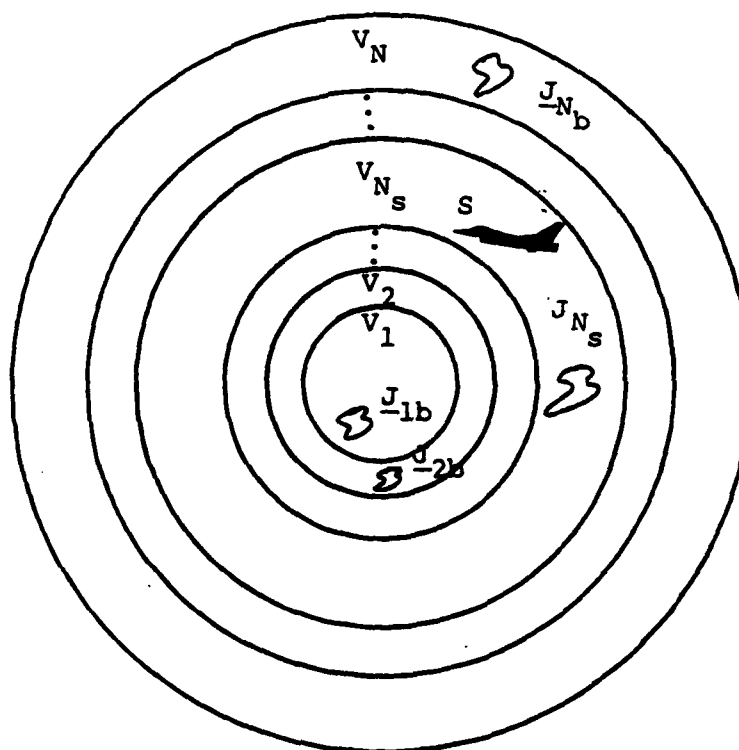


Figure 2b. Radially Stratified Medium Configuration

$$\underline{E}_{l\alpha}(\underline{r}) \equiv \underline{E}_l(\underline{r}, \underline{r}_\alpha) \quad (5a)$$

$$\underline{H}_{l\alpha}(\underline{r}) \equiv \underline{H}_l(\underline{r}, \underline{r}_\alpha) \quad (5b)$$

Whenever the sources are delta functions, we will consider the scattering body to be absent. We now use the vector identity

$$\nabla \cdot (\underline{A} \times \underline{B}) = \underline{B} \cdot (\nabla \times \underline{A}) - \underline{A} \cdot (\nabla \times \underline{B})$$

to obtain

$$\begin{aligned} \nabla \cdot (\underline{E}_{l\alpha} \times \underline{H}_{lb} - \underline{E}_{lb} \times \underline{H}_{la}) &= \underline{H}_{lb} \cdot \nabla \times \underline{E}_{la} - \underline{E}_{la} \cdot \nabla \times \underline{H}_{lb} \\ &\quad - (\underline{H}_{la} \cdot \nabla \times \underline{E}_{lb} - \underline{E}_{lb} \cdot \nabla \times \underline{H}_{la}) \end{aligned} \quad (6)$$

The quantities \underline{E}_{la} and \underline{H}_{la} satisfy Equations 1 and 2 for $\alpha=a$, and similarly \underline{E}_{lb} and \underline{H}_{lb} satisfy Equations 1 and 2 for $\alpha=b$. Substituting these versions of Equations 1 and 2 into the right-hand side of Equation 6 and then cancelling terms, we obtain

$$\nabla \cdot \underline{D}_l = \underline{E}_{lb} \cdot \underline{J}_{la} - \underline{E}_{la} \cdot \underline{J}_{lb} \quad (7)$$

$$\underline{D}_l \equiv \underline{E}_{la} \times \underline{H}_{lb} - \underline{E}_{lb} \times \underline{H}_{la} \quad (8)$$

Integrating both sides of Equation 7 over V_l and employing the divergence theorem, we obtain

$$I_{sl, l-1} + I_{sl, l+1} + \delta_{l, N_s} I_s = I_{Vlba} - I_{Vlab} \quad (9)$$

where

$$I_{sl, k} \equiv \int_{S_{l, k}} \hat{n}_{l, k} \cdot \underline{D}_l dS \quad (10)$$

$$I_s \equiv \int_S \hat{n}_p \cdot \underline{D}_{N_s} dS \quad (11)$$

$$I_{V_{l\alpha\beta}} \equiv \int_{V_l} \underline{E}_{l\alpha} \cdot \underline{J}_{l\beta} dV \quad (12)$$

where $S_{l,k}$ is the surface interface between volumes V_l and V_k ; $\hat{n}_{l,k}$ is the normal to $S_{l,k}$ directed outward from V_l into V_k ; S is the surface of the perfectly conducting object which is embedded in V_{N_s} ; \hat{n}_p is the inward normal to S , and δ_{l,N_s} is the Kronecker delta function. In Appendix A it is argued that despite the absence of physical surfaces for $I_{s1,0}$ and $I_{sN,N+1}$, both integrals have zero value.

We now focus attention on Equation 9 for the situation where $l = N_s$; the only \underline{J}_{la} source is in V_{N_s} and has the form

$$\underline{J}_{N_s a} = \hat{a} \delta(\underline{r} - \underline{r}_a) \quad (13)$$

For this case, Equation 9 becomes

$$F_{N_s ab} + I_s = \hat{a} \cdot \underline{E}_{N_s b}(\underline{r}_a) \quad (14)$$

$$\text{where } F_{N_s ab} \equiv I_{sN_s, N_s-1} + I_{sN_s, N_s+1} + I_{VN_s ab} \quad (15)$$

In Appendix A, it will be shown that $F_{N_s ab}$ is independent of the presence (or absence) of the embedded perfect conductor for a general distribution of \underline{J}_{lb} 's, and this proof will utilize Equation 9 for l not being restricted to N_s . Using the fact that $F_{N_s ab}$ does not depend on the scattering object, we will give this quantity explicit meaning. We return to Equations 13 and 14 and consider that we sequentially introduce the following three sources all located at \underline{r}_a

$$\underline{J}_{N_s a}^i = \hat{a}_i \delta(\underline{r} - \underline{r}_a) \quad i=1,2,3 \quad (16)$$

with $(\hat{a}_1, \hat{a}_2, \hat{a}_3)$ forming an orthonormal set, and for each i we obtain, in the same manner that Equation 14 followed from Equation 13, the relation

$$F_{N_s ab}^i + I_s^i = \hat{a}_i \cdot \underline{E}_{N_s ab} \quad (17a)$$

where

$$\underline{E}_{N_s ab} \equiv \underline{E}_{N_s b}(\underline{r}_a) \quad (17b)$$

Utilizing the independence of the unit vectors, we rewrite this set of equations as a single vector equation.

$$\begin{aligned} \underline{F}_{N_s ab} + \underline{I}_s &= \hat{a}_1 (\hat{a}_1 \cdot \underline{E}_{N_s ab}) \\ &+ \hat{a}_2 (\hat{a}_2 \cdot \underline{E}_{N_s ab}) \\ &+ \hat{a}_3 (\hat{a}_3 \cdot \underline{E}_{N_s ab}) \end{aligned} \quad (18)$$

where

$$\underline{F}_{N_s ab} \equiv \hat{a}_1 F_{N_s ab}^1 + \hat{a}_2 F_{N_s ab}^2 + \hat{a}_3 F_{N_s ab}^3 \quad (19)$$

and

$$\underline{I}_s \equiv \hat{a}_1 I_s^1 + \hat{a}_2 I_s^2 + \hat{a}_3 I_s^3 \quad (20)$$

The right-hand side of Equation 18 can be interpreted by noting that the identity dyadic $\underline{\underline{I}}$ is expressible in terms of the set $(\hat{a}_1, \hat{a}_2, \hat{a}_3)$ as

$$\underline{\underline{I}} = \hat{a}_1 \hat{a}_1 + \hat{a}_2 \hat{a}_2 + \hat{a}_3 \hat{a}_3 \quad (21)$$

so that

$$\begin{aligned} \hat{a}_1 (\hat{a}_1 \cdot \underline{E}_{N_s ab}) + \hat{a}_2 (\hat{a}_2 \cdot \underline{E}_{N_s ab}) + \hat{a}_3 (\hat{a}_3 \cdot \underline{E}_{N_s ab}) \\ = \underline{\underline{I}} \cdot \underline{E}_{N_s ab} = \underline{E}_{N_s ab} \end{aligned} \quad (22)$$

and Equation 18 becomes

$$\underline{F}_{N_s ab} + \underline{I}_s = \underline{E}_{N_s ab} \quad (23)$$

Using the fact that $\underline{F}_{N_s ab}$ is independent of S , we consider the special case of Equation 23 where S vanishes and in turn \underline{I}_s vanishes, so that

$$\underline{F}_{N_s ab} = \underline{E}_{TN_s b}(\underline{r}_a) = \underline{E}_{TN_s ab} \quad (24)$$

with $\underline{E}_{TN_s ab}$ being the total electric field at \underline{r}_a excited by a general distribution of sources \underline{J}_{lb} . \underline{E}_{TN_s} includes all multiple scattering effects due to the stratified medium but does not include any scattering due to the embedded perfect conductor. We now write Equation 23 as

$$\underline{E}_{N_s b}(\underline{r}_a) = \underline{E}_{TN_s b}(\underline{r}_a) + \underline{I}_s \quad (25)$$

We now focus our attention on \underline{I}_s and express Equation 20 in more detail

$$\underline{I}_s = \sum_{i=1}^3 \int_s (\hat{n}_p \cdot \underline{D}_{Ns}^i) \hat{a}_i dS \quad (26)$$

with

$$\underline{D}_{Ns}^i = \underline{E}_{Ns}^i \times \underline{H}_{Ns}^i b - \underline{E}_{Ns}^i b \times \underline{H}_{Ns}^i a \quad (27)$$

Forming $\hat{n}_p \cdot \underline{D}_{Ns}^i$ and using standard triple scalar product manipulations, we obtain

$$\hat{n}_p \cdot \underline{D}_{Ns}^i = -(\hat{n}_p \times \underline{H}_{Ns}^i b) \cdot \underline{E}_{Ns}^i a - (\hat{n}_p \times \underline{E}_{Ns}^i b) \cdot \underline{H}_{Ns}^i a \quad (28)$$

The boundary conditions require that the tangential electric field excited by the \underline{J}_{lb} 's on the embedded conductor vanishes so the second term in Equation 28 vanishes. We note in passing, that we cannot apply the same argument to eliminate the first term since the scattering body is absent in the "a" system. Equation 28 is now written as

$$\hat{n}_p \cdot \underline{D}_{Ns}^i = \underline{J}(\underline{r}) \cdot \underline{E}_{Ns}^i a \quad (29)$$

In order to obtain this equation, we used the fact that the surface current on S excited by the \underline{J}_{lb} 's is given by

$$\underline{J}(\underline{r}) = \hat{n}_o \times \underline{H}_{Ns} b \quad (30)$$

with $\hat{n}_p = -\hat{n}_o$ and \hat{n}_o is the outward normal to S. Combining Equations 25, 26, and 29, we obtain

$$\underline{E}_{Ns} b(\underline{r}_a) = \underline{E}_{TNs} b(\underline{r}_a) + \int_s \underline{J}(\underline{r}) \cdot \underline{G}_{Ns}(\underline{r}, \underline{r}_a) dS \quad (31)$$

where

$$\underline{\underline{G}}_{N_s}(\underline{r}, \underline{r}_a) = \sum_{i=1}^3 \underline{\underline{E}}_{N_s}^i(\underline{r}, \underline{r}_a) \hat{a}_i \quad (32)$$

Equation 31 has many of the properties we were seeking in that it is a representation of the fields excited by general sources in a stratified medium having an embedded conductor; the presence of the conductor is accounted for by the surface integral. Furthermore, this surface integral contains a Green's dyadic that can be explicitly formed in the described manner, i.e. using the three electric field representations generated by three orthonormal dipole sources. Despite these features of Equation 31, it is not the final form desired because the Green's dyadic appears to be the right of $\underline{J}(\underline{r})$, and this form does not readily allow us to take the curl of both sides of the equation. The significance is that this is the procedure used to obtain a surface integral representation for $\underline{H}_\ell(\underline{r})$.

Returning to Equation 31, we use the following property valid for any dyadic $\underline{\underline{D}}$ and vector \underline{V}

$$\underline{V} \cdot \underline{\underline{D}} = \tilde{\underline{\underline{D}}} \cdot \underline{V} \quad (33)$$

where $\tilde{\underline{\underline{D}}}$ is the transpose of $\underline{\underline{D}}$. The surface integral in Equation 31 is now written as

$$\int_s \underline{J}(\underline{r}) \cdot \underline{\underline{G}}_{N_s}(\underline{r}, \underline{r}_a) dS = \int_s \tilde{\underline{\underline{G}}}_{N_s}(\underline{r}, \underline{r}_a) \cdot \underline{J}(\underline{r}) dS \quad (34)$$

In Appendix B we will prove that

$$\tilde{\underline{\underline{G}}}_j(\underline{r}, \underline{r}_a) = \underline{\underline{G}}_k(\underline{r}_a, \underline{r}) \quad \underline{r} \in V_j, \underline{r}_a \in V_k \quad (35)$$

Combining Equations 31, 34, and 35, we obtain

$$\underline{E}_{N_s b}(\underline{r}_a) = \underline{E}_{TN_s b}(\underline{r}_a) + \int_s \underline{G}_{N_s}(\underline{r}_a, \underline{r}) \cdot \underline{J}(\underline{r}) dS \quad (36)$$

which is our desired representation for the electric field. Next we introduce a notation change in order to make this equation conform to standard notation for integration and observation variables; i.e., \underline{r} is typically used for the observation variable and \underline{r}' for the integration. The distinction between \underline{r} and \underline{r}' is more than just notation in that \underline{r} must be interpretable as ranging over a three-dimensional volume while \underline{r}' is restricted to range over the two-dimensional surface of the scattering object. Denoting the volume variable in Equation 36 as \underline{r} and the surface variable as \underline{r}' and dropping the explicit "b" notational dependence, we rewrite that equation as

$$\underline{E}_{N_s}(\underline{r}) = \underline{E}_{TN_s}(\underline{r}) + \int_s \underline{G}_{N_s}(\underline{r}, \underline{r}') \cdot \underline{J}(\underline{r}') dS' \quad (37)$$

Before we elaborate on the meaning of this representation, we claim that the representation is valid for general values of ℓ ; and for general ℓ , we have

$$\underline{E}_\ell(\underline{r}) = \underline{E}_{T\ell}(\underline{r}) + \int_s \underline{G}_\ell(\underline{r}, \underline{r}') \cdot \underline{J}(\underline{r}') dS' \quad (38)$$

The essential details of how Equation 38 is derived for $\ell \neq N_s$ is presented in Appendix C. The reason that we focus on the case $\ell = N_s$ is that it is this case that leads to the explicit equation that we numerically solve to determine $\underline{J}(\underline{r})$.

A discussion of the meaning of Equation 38 requires that we return to the definition of \underline{G}_ℓ given by Equation 32. Without restricting ℓ , we use the arguments leading to that equation to express $\underline{G}_\ell(\underline{r}, \underline{r}')$ as

$$\underline{G}_\ell(\underline{r}, \underline{r}') = \sum_{i=1}^3 \underline{E}_\ell^i(\underline{r}, \underline{r}') \hat{a}_i \quad (39)$$

with $\underline{E}_\ell^i(\underline{r}, \underline{r}')$ satisfying the boundary conditions described in Appendix A as well as the equations

$$\nabla \times \underline{E}_\ell^i(\underline{r}, \underline{r}') = i\omega\mu_\ell \underline{H}_\ell^i(\underline{r}, \underline{r}') \quad (40)$$

$$\nabla \times \underline{H}_\ell^i(\underline{r}, \underline{r}') = -i\omega\epsilon_\ell \underline{E}_\ell^i(\underline{r}, \underline{r}') + \hat{a}_i \delta(\underline{r} - \underline{r}') \quad (41)$$

In these equations \underline{r} is the variable ranging over a three-dimensional space, V_ℓ , and the curl appearing in these equations operates with respect to this variable. The \underline{r}' pertains to the location of the dipole source, and it is chosen to lie in the same volume as the embedded scatterer. It is oriented in the \hat{a}_i direction with the choice of these orientations being such that $(\hat{a}_1, \hat{a}_2, \hat{a}_3)$ form an orthonormal set. To complete the description of Equation 38, we simply state that $\underline{E}_{T\ell}(\underline{r})$ is the total electric field at \underline{r} , which includes all multiple scattering due to the stratification of the medium, but considers the embedded conductor to be removed.

Next we obtain a representation for the magnetic field in terms of the surface integral by taking the curl with respect to the \underline{r} variables of both sides of Equation 38 to obtain

$$\nabla \times \underline{E}_\ell(\underline{r}) = \nabla \times \underline{E}_{T\ell}(\underline{r}) + \int_S \nabla \times \underline{G}_\ell(\underline{r}, \underline{r}') \cdot \underline{J}(\underline{r}') dS \quad (42)$$

Using Equation 1 for the special case $\alpha = b$ and considering the scattering object to be present, we would be able to conclude that

$$\nabla \times \underline{E}_\ell(\underline{r}) = i\omega\mu_\ell \underline{H}_\ell(\underline{r}) \quad (43)$$

or considering the object to be absent, we would be able to conclude that

$$\nabla \times \underline{E}_{T\ell}(\underline{r}) = i\omega\mu_{\ell}\underline{H}_{T\ell}(\underline{r}) \quad (44)$$

Now defining

$$i\omega\mu_{\ell}\underline{K}_{\ell}(\underline{r},\underline{r}') = \nabla \times \underline{G}_{\ell}(\underline{r},\underline{r}') \quad (45)$$

we can rewrite Equation 42 as

$$\underline{H}_{\ell}(\underline{r}) = \underline{H}_{T\ell}(\underline{r}) + \int_S \underline{K}_{\ell}(\underline{r},\underline{r}') \cdot \underline{J}(\underline{r}') dS' \quad (46)$$

We obtain our final expression for \underline{K}_{ℓ} by combining Equations 39, 40, and 44 which results in

$$\underline{K}_{\ell}(\underline{r},\underline{r}') = \sum_{i=1}^3 \underline{H}_{\ell}^i(\underline{r},\underline{r}') \hat{a}_i \quad (47)$$

Equations 38 and 46 are the desired surface integral representations and Equations 39, 40, 41, and 47 are the equations that give these representations utility. In the next section we will give Equations 39 and 40 explicit meaning for a two-layered medium, and in the following section we will obtain the EFIE and the MFIE by discussing the limit of Equations 38 and 46 as \underline{r} approaches the surface.

III. EXPLICIT GREEN'S DYADIC REPRESENTATIONS FOR THE TWO-LAYERED CONFIGURATION OF INTEREST

In this section we will obtain explicit representations for $\underline{\underline{G}}_\ell(\underline{r}, \underline{r}')$ and $\underline{\underline{K}}_\ell(\underline{r}, \underline{r}')$ using the prescription summarized by Equations 39, 40, 41, and 47 with the boundary conditions described in Appendix A also being satisfied. These representations will be found for the case where we have a two-layered horizontally stratified medium with one layer being a lossy half-space, $\ell=1$, and the other layer being a vacuum half-space, $\ell=2$. Our scattering object is in V_2 , and we will focus our attention on obtaining the explicit representations for $\underline{\underline{G}}_2(\underline{r}, \underline{r}')$ and $\underline{\underline{K}}_2(\underline{r}, \underline{r}')$. We will present these representations in a form where it is clear that they are identical to representations of the same dyadics that were obtained by a different formalism (Reference 1). We obtain our explicit representations by utilizing representations contained in the book by Baños (Reference 3) for the electric fields and the magnetic fields excited in the vacuum half-space above a lossy half-space by horizontal and vertical electric dipoles located in the vacuum region.

In order to use Baños's explicit results, it is necessary to employ a systematic bookkeeping procedure to compensate for the choice of coordinate system chosen by Baños, which was convenient for his purposes but not ours. Specifically, Baños gives explicit solutions, that we will denote $\underline{E}_{B2}^i(\underline{r}_D, \underline{r}'_D)$ and $\underline{H}_{B2}^i(\underline{r}_D, \underline{r}'_D)$ which satisfy the equations

$$\nabla_D \times \underline{E}_{B2}^i(\underline{r}_D, \underline{r}'_D) = i\omega\mu_2 \underline{H}_{B2}^i(\underline{r}_D, \underline{r}'_D) \quad (48)$$

$$\nabla_D \times \underline{H}_{B2}^i(\underline{r}_D, \underline{r}'_D) = -i\omega\epsilon_2 \underline{E}_{B2}^i(\underline{r}_D, \underline{r}'_D) + p \hat{a}_i \delta(\underline{r}_D - \underline{r}'_D) \quad (49)$$

and it is necessary to augment the solutions to these equations for two reasons in order to obtain the $\underline{E}_2^i(\underline{r}, \underline{r}')$ and $\underline{H}_2^i(\underline{r}, \underline{r}')$ required by Equations 39 and 47. One reason is that Baños chooses a coordinate system in which \underline{r}_D' is allowed to vary only over one linear dimension rather than the necessary three, and the other is that he presents explicit solutions for only two orthonormal vectors $\hat{a}_1 = \hat{a}_x$, and $\hat{a}_3 = \hat{a}_z$. Despite these limitations, the necessary solutions can readily be obtained from $\underline{E}_{B2}^{1,3}$ and $\underline{H}_{B2}^{1,3}$.

We now elaborate on the coordinate system used by Baños. The origin of that coordinate system lies on the interface, and the positive z-axis points into V_2 . The subscript D is not used by Baños but is introduced by us in order to distinguish between the variables used in the previous section from his variables. We use his result by obtaining $\underline{E}_{B2}^2(\underline{r}_D, \underline{r}_D')$ and $\underline{H}_{B2}^2(\underline{r}_D, \underline{r}_D')$ and then utilizing the following relationship

$$\underline{E}_2^i(\underline{r}, \underline{r}') = \frac{1}{p} \underline{E}_{B2}^i \left[\underline{r}_D(\underline{r}, \underline{r}'), \underline{r}_D(\underline{r}, \underline{r}') \right] \quad (50)$$

$$\underline{H}_2^i(\underline{r}, \underline{r}') = \frac{1}{p} \underline{H}_{B2}^i \left[\underline{r}_D(\underline{r}, \underline{r}'), \underline{r}_D'(\underline{r}, \underline{r}') \right] \quad (51)$$

In order to use Equations 50 and 51, it is necessary to determine the functional relationships

$$\underline{r}_D \equiv \underline{r}_D(\underline{r}, \underline{r}') \quad (52)$$

and

$$\underline{r}_D' \equiv \underline{r}_D'(\underline{r}, \underline{r}') \quad (53)$$

The description of how the coordinate functional relationships are obtained is facilitated by referring to Figure 3.

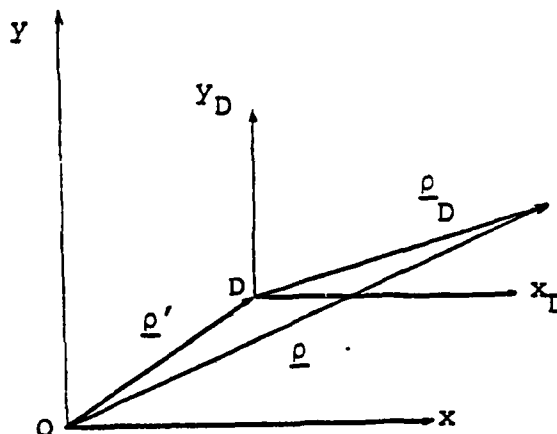


Figure 3. Coordinate Systems

This figure is the view of the $z = 0$ plane (the interface) for all coordinate descriptions of interest. Because of this choice of coordinates, it follows that

$$z_D = z \quad (54)$$

$$z_D' = z' \quad (55)$$

and we note that Baños uses the notation $z'_D = h$. The significance of choosing the coordinate system having the origin "O" in addition to the Baños coordinate system having the origin "D" is that the location of the dipole source is fixed in the "D" coordinate system at the origin but is free to vary in the "O" coordinate system. Also, its position is denoted $\underline{\rho}'$ in accord with the meaning of the primed coordinates described in the previous section. Still in accord with the meaning ascribed to the variables discussed in that section, $\underline{\rho}$ identifies the location of the observation point in the "O" coordinate system. From the construction of the two coordinate systems, we have the relationship

$$\underline{\rho}_D = \underline{\rho} - \underline{\rho}' \quad (56)$$

and the fact that $\underline{\rho}_D$ is the difference between the two coordinates of interest is the reason for designating Baños coordinates with the subscript "D". It should be noted that Baños denotes $\rho_D = |\underline{\rho}_D|$ as r in his book, and this should not be confused with $|\underline{r}|$ where we mean $\underline{r} = \underline{\rho} + z\hat{a}_z$. We now have determined the required coordinate functional relationships which can be summarized as

$$\underline{r}_D = \underline{\rho} - \underline{\rho}' + z\hat{a}_z \quad (57)$$

$$\underline{r}'_D = z'\hat{a}_z \quad (58)$$

We will now determine $\underline{E}_{B2}^2(\underline{r}_O, \underline{r}'_O)$ and $\underline{H}_{B2}^2(\underline{r}_O, \underline{r}'_O)$ in terms of the explicit expressions that Baños gives for $\underline{E}_{B2}^1(\underline{r}_O, \underline{r}'_O)$ and $\underline{H}_{B2}^1(\underline{r}_O, \underline{r}'_O)$. The derivation simplifies by noting that the spatial dependence of the latter quantities can be expressed in terms of the three scalars ρ_D , $z+z'$, and ϕ_D . Let us consider the situation described by the argument $(\rho_D, z+z', \phi_D + \pi/2)$

and the fields excited by an electric dipole located at the origin of the "D" coordinate system that is directed along $\hat{a}_y = \hat{a}_2$. The fields generated by the dipole are

$$\begin{aligned} \underline{E}_{B2}^2(\rho_D, z+z', \phi_D+\pi/2) &= E_{\rho B2}^2(\rho_D, z+z', \phi_D+\pi/2) \hat{a}_{\rho D}(\phi_D+\pi/2) \\ &+ E_{\phi B2}^2(\rho_D, z+z', \phi_D+\pi/2) \hat{a}_{\phi D}(\phi_D+\pi/2) \\ &+ E_{z B2}^2(\rho_D, z+z', \phi_D+\pi/2) \hat{a}_z \end{aligned} \quad (59)$$

The geometry of the physical situation is such that

$$E_{\rho B2}^2(\rho_D, z+z', \phi_D+\pi/2) = E_{\rho B2}^1(\rho_D, z+z', \phi_D) \quad (60a)$$

$$E_{\phi B2}^2(\rho_D, z+z', \phi_D+\pi/2) = E_{\phi B2}^1(\rho_D, z+z', \phi_D) \quad (60b)$$

$$E_{z B2}^2(\rho_D, z+z', \phi_D+\pi/2) = E_{z B2}^1(\rho_D, z+z', \phi_D) \quad (60c)$$

and it is worth noting that despite these relationships

$$\underline{E}_{B2}^2(\rho_D, z+z', \phi_D+\pi/2) \neq \underline{E}_{B2}^1(\rho_D, z+z', \phi_D)$$

because $\hat{a}_{\rho}(\phi_D+\pi/2) \neq \hat{a}_{\rho}(\phi_D)$, and $\hat{a}_{\phi}(\phi_D+\pi/2) \neq \hat{a}_{\phi}(\phi_D)$. The geometry arguments also apply for the magnetic field as well leading to the statement

$$H_{\alpha B2}^2(\rho_D, z+z', \phi_D+\pi/2) = H_{\alpha B2}^1(\rho_D, z+z', \phi_D) \quad \alpha=\rho, \phi, z \quad (61)$$

We now collect the appropriate results presented by Baños, change to the "D" notation, and use Equations 60 and 61 to obtain

$$E_{\rho B2}^1 = Q \cos \phi_D \left(\frac{\partial^2 A}{\partial \rho_D^2} + k_{2B}^2 \right) \quad (62)$$

$$E_{\phi B2}^1 = -Q \sin \phi_D \left(\frac{1}{\rho_D} \frac{\partial A}{\partial \rho_D} + k_{2B}^2 \right) \quad (63)$$

$$E_{zB2}^1 = Q \cos \phi_D \frac{\partial^2}{\partial z \partial \rho_D} (G_{22} + C) \quad (64)$$

$$H_{\rho B2}^1 = S \sin \phi_D \left(\frac{\partial B}{\partial z} - \frac{1}{\rho_D} \frac{\partial W_{22}}{\partial \rho_D} \right) \quad (65)$$

$$H_{\phi B2}^1 = S \cos \phi_D \left(\frac{\partial B}{\partial z} - \frac{\partial^2 W_{22}}{\partial \rho_D^2} \right) \quad (66)$$

$$H_{zB2}^1 = S \sin \phi_D \frac{\partial B}{\partial \rho_D} \quad (67)$$

$$E_{\rho B2}^2 = Q \sin \phi_D \left(\frac{\partial^2 A}{\partial \rho_D^2} + k_{2B}^2 \right) \quad (68)$$

$$E_{\phi B2}^2 = Q \cos \phi_D \left(\frac{1}{\rho_D} \frac{\partial A}{\partial \rho_D} + k_{2B}^2 \right) \quad (69)$$

$$E_{zB2}^2 = Q \sin \phi_D \frac{\partial^2}{\partial z \partial \rho_D} (G_{22} + C) \quad (70)$$

$$H_{\rho B2}^2 = -S \cos \phi_D \left(\frac{\partial B}{\partial z} - \frac{1}{\rho_D} \frac{\partial W_{22}}{\partial \rho_D} \right) \quad (71)$$

$$H_{\phi B2}^2 = S \sin \phi_D \left(\frac{\partial B}{\partial z} - \frac{\partial^2 W_{22}}{\partial \rho_D^2} \right) \quad (72)$$

$$H_{zB2}^2 = S \cos \phi_D \frac{\partial B}{\partial \rho_D} \quad (73)$$

$$E_{\rho B2}^3 = Q \frac{\partial^2}{\partial z \partial \rho_D} (G_{22} - C) \quad (74)$$

$$E_{\phi B2}^3 = H_{\rho B2}^3 = H_{zB2}^3 = 0 \quad (75)$$

$$E_{zB2}^3 = Q \left(\frac{\partial^2}{\partial z^2} + k_2^2 \right) (G_{22} - C) \quad (76)$$

$$H_{\phi B2}^3 = -S \frac{\partial}{\partial \rho} (G_{22} - C) \quad (77)$$

where

$$Q = \frac{i\omega\mu_2}{4\pi k_2^2} \quad (78)$$

$$S = \frac{p}{4\pi} \quad (79)$$

$$k_\ell^2 = \omega^2 \mu_\ell \epsilon_\ell \quad (80)$$

$$A = G_{22} - G_{21} + k_2^2 V_{22} \quad (81)$$

$$B = G_{22} - G_{21} + U_{22} \quad (82)$$

$$C = G_{21} - k_1^2 V_{22} \quad (83)$$

$$G_{22} = R^{-1} e^{ik_2 R} \quad (84)$$

$$G_{21} = R_+^{-1} e^{ik_2 R_+} \quad (85)$$

$$R = \left(\rho_D^2 + (z-z')^2 \right)^{1/2} \quad (86)$$

$$R_+ = \left(\rho_D^2 + (z+z')^2 \right)^{1/2} \quad (87)$$

$$U_{22} = \int_0^\infty \frac{2e^{-\gamma_2(z+z')}}{\gamma_1 + \gamma_2} J_0(\lambda \rho_D) \lambda d\lambda \quad (88)$$

$$V_{22} = \int_0^\infty \frac{2e^{-\gamma_2(z+z')}}{k_2^2 \gamma_1 + k_1^2 \gamma_2} J_0(\lambda \rho_D) \lambda d\lambda \quad (89)$$

$$W_{22} = \int_0^\infty \frac{2(\gamma_1 - \gamma_2) e^{-\gamma_2(z+z')}}{k_2^2 \gamma_1 + k_1^2 \gamma_2} J_0(\lambda \rho_D) \lambda d\lambda \quad (90)$$

$$\gamma_{\ell} = (\lambda^2 - k_{\ell}^2)^{1/2} \quad (91)$$

The variety of branch cuts that have been used to define γ_{ℓ} are discussed by Baños. We are now in a position to utilize Equations 50 and 51 to obtain $\underline{E}_2^i(\underline{r}, \underline{r}')$ and $\underline{H}_2^i(\underline{r}, \underline{r}')$ and then in turn to use Equations 39 and 47 to obtain the desired quantities $\underline{G}_2(\underline{r}, \underline{r}')$ and $\underline{K}_2(\underline{r}, \underline{r}')$. Following this procedure, we obtain

$$\underline{G}_2(\underline{r}, \underline{r}') = i\omega\mu_2 \left[\underline{G}_0(\underline{r}, \underline{r}') + \underline{G}_s(\underline{r}, \underline{r}') \right] \quad (92)$$

$$\underline{K}_2(\underline{r}, \underline{r}') = \underline{K}_0(\underline{r}, \underline{r}') + \underline{K}_s(\underline{r}, \underline{r}') \quad (93)$$

where

$$\begin{aligned} 4\pi k_2^2 \underline{G}_{\beta}(\underline{r}, \underline{r}') = & G_{\beta\rho\rho} \hat{a}_{\rho_D} \hat{a}_{\rho_D} + G_{\beta\phi\phi} \hat{a}_{\phi_D} \hat{a}_{\phi_D} + G_{\beta\rho z} \hat{a}_{\rho_D} \hat{a}_z \\ & + G_{\beta z\rho} \hat{a}_z \hat{a}_{\rho_D} + G_{\beta z z} \hat{a}_z \hat{a}_z \quad \beta=0, s \end{aligned} \quad (94)$$

$$\begin{aligned} 4\pi \underline{K}_{\beta}(\underline{r}, \underline{r}') = & K_{\beta\rho\phi} \hat{a}_{\rho_D} \hat{a}_{\phi_D} + K_{\beta\phi\rho} \hat{a}_{\phi_D} \hat{a}_{\rho_D} \\ & + K_{\beta z\phi} \hat{a}_z \hat{a}_{\phi_D} + K_{\beta\phi z} \hat{a}_{\phi_D} \hat{a}_z \quad \beta=0, s \end{aligned} \quad (95)$$

$$G_{0\rho\rho} = \frac{\partial^2 G_{22}}{\partial \rho_D^2} + k_2^2 G_{22} \quad (96)$$

$$G_{\phi\phi} = \frac{1}{\rho_D} \frac{\partial G_{22}}{\partial \rho_D} + k_2^2 G_{22} \quad (97)$$

$$G_{\phi z} = \frac{\partial^2 G_{22}}{\partial \rho_D \partial z} = G_{z\phi} \quad (98)$$

$$G_{zz} = \frac{\partial^2 G_{22}}{\partial z^2} + k_2^2 G_{22} \quad (99)$$

$$G_{\rho\rho} = \frac{\partial^2}{\partial \rho_D^2} (-G_{21} + k_2^2 V_{22}) + k_2^2 (-G_{21} + U_{22}) \quad (100)$$

$$G_{\phi\phi} = \frac{1}{\rho_D} \frac{\partial}{\partial \rho_D} (-G_{21} + k_2^2 V_{22}) + k_2^2 (-G_{21} + U_{22}) \quad (101)$$

$$G_{\rho z} = \frac{\partial^2}{\partial \rho_D \partial z} (-G_{21} + k_1^2 V_{22}) = -G_{z\rho} \quad (102)$$

$$G_{zz} = \left(\frac{\partial^2}{\partial z^2} + k_2^2 \right) (-G_{21} + k_1^2 V_{22}) \quad (103)$$

$$K_{\phi\phi} = \frac{-\partial G_{22}}{\partial z} = -K_{\phi\rho} \quad (104)$$

$$K_{\phi z} = \frac{\partial G_{22}}{\partial \rho} = -K_{\phi z} \quad (105)$$

$$K_{\rho\phi} = \frac{\partial}{\partial z} (G_{21} - U_{22}) + \frac{1}{\rho_D} \frac{\partial W_{22}}{\partial \rho_D} \quad (106)$$

$$K_{s\phi\rho} = \frac{\partial}{\partial z} \left(-G_{21} + U_{22} \right) - \frac{\partial^2 W_{22}}{\partial \rho_D^2} \quad (107)$$

$$K_{sz\phi} = \frac{\partial}{\partial \rho_D} \left(-G_{21} + U_{22} \right) \quad (108)$$

$$K_{s\phi z} = \frac{\partial}{\partial \rho_D} \left(G_{21} - k_1^2 V_{22} \right) \quad (109)$$

After making the described substitutions, it was necessary to use the coordinate relationships

$$\hat{a}_{\rho_D} = \hat{a}_x \cos \phi_D + \hat{a}_y \sin \phi_D \quad (110)$$

and

$$\hat{a}_{\phi_D} = -\hat{a}_x \sin \phi_D + \hat{a}_y \cos \phi_D \quad (111)$$

in order to obtain Equation 92 through Equation 109. Even though the explicit representations for \hat{a}_{ρ_D} and \hat{a}_{ϕ_D} given by Equations 110 and 111 were used to obtain the expressions for $\underline{G}_2(\underline{r}, \underline{r}')$ and $\underline{K}_2(\underline{r}, \underline{r}')$, it may be more convenient to use the final expressions with alternate representations for the unit vector as expressed in the "O" coordinate system. From Equation 56 it follows that

$$\hat{a}_{\rho_D} = \frac{\rho - \rho'}{\rho_D} \quad (112)$$

and from the properties of the orthonormal set $(\hat{a}_{\rho_D}, \hat{a}_{\phi_D}, \hat{a}_z)$, it follows that

$$\hat{a}_{\phi_D} = \hat{a}_z \times \frac{\rho - \rho'}{\rho_D} \quad (113)$$

We now note that the $\underline{\underline{K}}_s(\underline{r}, \underline{r}')$ and $\underline{\underline{G}}_s(\underline{r}, \underline{r}')$ derived in this section are identical to the corresponding quantities presented in Reference 1 which were derived by a different method. To complete the comparison with the material presented in that reference, we note that by simply performing the derivatives indicated in the representations presented in that reference

$$4\pi \underline{\underline{G}}_o(\underline{r}, \underline{r}') = \left(\underline{\underline{I}} + k_2^{-2} \nabla \nabla \right) G_{22} \quad (114)$$

and

$$4\pi \underline{\underline{K}}_o(\underline{r}, \underline{r}') = \nabla G_{22} \times \underline{\underline{I}} \quad (115)$$

it follows that these expressions are identical with $\underline{\underline{G}}_o$ and $\underline{\underline{K}}_o$ presented in this section. Finally, we note that the significance of the representations presented in Equations 114 and 115 will be seen in a subsequent section when we are concerned with the limit as \underline{r} approaches the surface.

IV. EXPLICIT REPRESENTATIONS FOR $\underline{E}_T(\underline{r})$ AND $\underline{H}_T(\underline{r})$
FOR THE TWO-LAYERED PROBLEM OF INTEREST

In this section we will present the same results that were presented in Reference 1; however, we will rewrite those expressions in a form where it is possible to readily make a very important observation. We will restrict our attention to the case where the incident field is a plane wave given by

$$\underline{E}_i = \hat{e} E_0 e^{ik_2 \hat{n}_0 \cdot \underline{r}} \quad (116)$$

with \hat{e} being a unit vector along the polarization direction and \hat{n}_0 being a unit vector in the propagation direction. Rewriting the expressions for \underline{E}_T and \underline{H}_T given in Reference 1, we have

$$E_0^{-1} \underline{E}_T(\underline{r}) = (\hat{e} \cdot \hat{h}) \hat{h} \psi + (\hat{e} \cdot \hat{v}) \left[\hat{v} \phi + 2 \left(\phi - e^{ik_2 \hat{n}_0 \cdot \underline{r}} \right) (\hat{n}_0 \cdot \hat{a}_z) (\hat{a}_z \times \hat{h}) \right] \quad (117)$$

$$z_2 E_0^{-1} \underline{H}_T(\underline{r}) = (\hat{e} \cdot \hat{v}) \hat{h} \phi - (\hat{e} \cdot \hat{h}) \left[\hat{v} \psi + 2 \left(\psi - e^{ik_2 \hat{n}_0 \cdot \underline{r}} \right) (\hat{n}_0 \cdot \hat{a}_z) (\hat{a}_z \times \hat{h}) \right] \quad (118)$$

where

$$z_2 = \sqrt{\frac{\mu_2}{\epsilon_2}} \quad (119)$$

$$\psi = e^{ik_2 \hat{n}_0 \cdot \underline{r}} + R_H e^{ik_2 \hat{n}_0 R \cdot \underline{r}} \quad (120)$$

$$\phi = e^{ik_2 \hat{n}_0 \cdot \underline{r}} + R_V e^{ik_2 \hat{n}_0 R \cdot \underline{r}} \quad (121)$$

$$\hat{n}_{OR} = \hat{n}_O - 2\hat{a}_z (\hat{a}_z \cdot \hat{n}_O) \quad (122)$$

$$\hat{h} = \frac{\hat{n}_O \times \hat{a}_z}{|\hat{n}_O \times \hat{a}_z|} \quad (123)$$

$$\hat{v} = \hat{h} \times \hat{n}_O \quad (124)$$

$$R_H = \frac{-k_2 (\hat{a}_z \cdot \hat{n}_O) - \{k_1^2 - k_2^2 [1 - (\hat{a}_z \cdot \hat{n}_O)^2]\}^{1/2}}{-k_2 (\hat{a}_z \cdot \hat{n}_O) + \{k_1^2 - k_2^2 [1 - (\hat{a}_z \cdot \hat{n}_O)^2]\}^{1/2}} \quad (125)$$

$$R_V = \frac{-k_1^2 (\hat{a}_z \cdot \hat{n}_O) - k_2 \{k_1^2 - k_2^2 [1 - (\hat{a}_z \cdot \hat{n}_O)^2]\}^{1/2}}{-k_1^2 (\hat{a}_z \cdot \hat{n}_O) + k_2 \{k_1^2 - k_2^2 [1 - (\hat{a}_z \cdot \hat{n}_O)^2]\}^{1/2}} \quad (126)$$

We can now discuss two important limiting cases of \underline{E}_T and \underline{H}_T . One is the limit as the conductivity of medium 1 becomes infinite ($k_1 \rightarrow \infty$), and the other is the limit as the incident angle becomes grazing ($\hat{a}_z \cdot \hat{n}_O \rightarrow 0$). In the infinite conductivity limit, we have

$$\lim_{k_1 \rightarrow \infty} R_H = -1 \quad (127)$$

$$\lim_{k_1 \rightarrow \infty} R_V = 1 \quad (128)$$

and in the grazing angle limit, we have

$$\lim_{(\hat{a}_z \cdot \hat{n}_O) \rightarrow 0} R_H = -1 \quad (129)$$

$$\lim_{(\hat{a}_z \cdot \hat{n}_O) \rightarrow 0} R_V = -1 \quad (130)$$

The difference in sign in the two limits expressed by Equations 128 and 130 leads to considerably different behavior for the total fields in these two limits. An important case to consider is the situation where the observation point above the ground is considerably less than the free-space wavelength so that $k_2 z \ll 1$. For this case, we choose a convenient coordinate system so that $\rho = 0$. We can approximate both $e^{ik_2 \hat{n}_O \cdot \underline{r}}$ and $e^{ik_2 \hat{n}_O R \cdot \underline{r}}$ by 1, so that under this restriction on observation height we have

$$\lim_{k_1 \rightarrow \infty} \psi = 0 \quad (131)$$

$$\lim_{k_1 \rightarrow \infty} \phi = 2 \quad (132)$$

$$\lim_{(\hat{a}_z \cdot \hat{n}_O) \rightarrow 0} \psi = 0 \quad (133)$$

$$\lim_{(\hat{a}_z \cdot \hat{n}_O) \rightarrow 0} \phi = 0 \quad (134)$$

Using Equations 131 through 134, we have under the restriction $k_2 z \ll 1$ the following

$$\lim_{k_1 \rightarrow \infty} E_O^{-1} \underline{E}_T(0+) = 2(\hat{e} \cdot \hat{v}) [\hat{v} + (\hat{n}_O \cdot \hat{a}_z)(\hat{a}_z \times \hat{h})] \quad (135)$$

$$\lim_{k_1 \rightarrow \infty} Z_2 E_O^{-1} \underline{H}_T(0+) = 2(\hat{e} \cdot \hat{v}) \hat{h} \quad (136)$$

which after algebraic manipulation can be written as

$$\lim_{k_1 \rightarrow \infty} E_O^{-1} \underline{E}_T(0+) = 2(\hat{a}_z \cdot \hat{e}) \hat{a}_z \quad (137)$$

$$\lim_{k_1 \rightarrow \infty} Z_2 E_O^{-1} \underline{H}_T(0+) = 2[(\hat{n}_O \times \hat{e}) \cdot \hat{h}] \hat{h} \quad (138)$$

Equations 137 and 138 are readily interpreted as representing the expected results for a perfect conductor, i.e., a doubling of both the normal incident electric field and the incident tangential magnetic field with all other components vanishing. The grazing angle limits are given by

$$\lim_{(\hat{n}_O \cdot \hat{a}_z) \rightarrow \infty} E_O^{-1} \underline{E}_T(0+) = 0 \quad (139)$$

$$\lim_{(\hat{n}_O \cdot \hat{a}_z) \rightarrow \infty} Z_2 E_O^{-1} \underline{H}_T(0+) = 0 \quad (140)$$

The implications of the extremely different limits of the perfectly conducting limits and the grazing angle limits are important to note. For the purposes of the numerical calculations performed in this report, we note that the induced

current density on an object above a lossy half-space or above a perfectly conducting ground will be significantly different for grazing incidence excitation. More important, questions having significant implications arise as a result of the difference between these limits. An immediate question is to what extent will a multilayered model of the earth and its atmosphere reduce the ground coverage of an EMP. Another question is how is this effect accounted for in one of the dominant EMP coupling mechanisms, i.e., the near grazing excitation of long lines above the earth. Finally, how do we interpret past ground-based system level tests where the intended exposure was grazing incidence?

V. PRESENTATION OF THE MAGNETIC FIELD INTEGRAL EQUATION (MFIE) AND THE ELECTRIC FIELD INTEGRO-DIFFERENTIAL EQUATION (EFIDE) FOR THE STRATIFIED MEDIUM SCATTERING PROBLEM

The essential details in arriving at the MFIE and the EFIDE for the stratified medium scattering problem are related to the examination of the limit as the observation point variable \underline{r} approaches the surface of the embedded scatterer. Specifically, we are interested in the

limit $\hat{n}_o(\underline{r}) \times \underline{E}_{N_s}(\underline{r}_v)$ and $\hat{n}_o(\underline{r}) \times \underline{H}_{N_s}(\underline{r}_v)$ where the $\underline{r}_v \rightarrow \underline{r}$ meaning of $\hat{n}_o(\underline{r})$, \underline{r} , and \underline{r}_v will be explained. The expressions for $\underline{E}_{N_s}(\underline{r}_v)$ and $\underline{H}_{N_s}(\underline{r}_v)$ are

$$\underline{E}_{N_s}(\underline{r}_v) = \underline{E}_{TN_s}(\underline{r}_v) + \int_s \underline{G}_{N_s}(\underline{r}_v, \underline{r}') \cdot \underline{J}(\underline{r}') dS' \quad (141)$$

and

$$\underline{H}_{N_s}(\underline{r}_v) = \underline{H}_{TN_s}(\underline{r}_v) + \int_s \underline{K}_{N_s}(\underline{r}_v, \underline{r}') \cdot \underline{J}(\underline{r}') dS' \quad (142)$$

Equation 141 is Equation 37 with the \underline{r} variable relabelled \underline{r}_v , and Equation 142 is Equation 46 for the case $l = N_s$, again with the \underline{r} variable relabelled \underline{r}_v . The reason for relabelling the observation variable is to emphasize that \underline{r}_v is allowed to vary over a three-dimensional volume as opposed to a two-dimensional surface. We reserve the variable \underline{r} to represent a variable related to \underline{r}_v but which is restricted to the surface of the scatterer. In general, this relationship is expressed as

$$\underline{r}_v = \underline{r} + \underline{q} \quad (143)$$

and we are interested in the behavior of Equations 141 and 142 as $|q| = q$ approaches zero. For many situations of interest we can argue that the angle at which \underline{r}_v approaches \underline{r} does not change the resulting equations and conveniently we choose

$$q = q\hat{n}_o(\underline{r}) \quad (144)$$

where $\hat{n}_o(\underline{r})$ is the outward normal to the scattering surface at point \underline{r} . For cases where Equation 144 is not applicable (e.g., \underline{r} corresponds to a tip or edge), it is still true that the stratified medium problem needs to be treated in exactly the same manner as the standard free-space MFIE and EFIE limits. Whether or not we can employ Equation 144, we will assume that a unique relationship can be specified between any point \underline{r} on the surface and a point \underline{r}_v in the proximity of the surface which is described by Equation 143 so that

$$\lim_{|q| \rightarrow 0} \underline{r}_v = \underline{r}$$

We can now express the limits of interest as

$$\begin{aligned} \lim_{q \rightarrow 0} \hat{n}_o(\underline{r}) \times \underline{E}_{N_s}(\underline{r}_v) &= \lim_{q \rightarrow 0} \hat{n}_o(\underline{r}) \times \underline{E}_{TN_s}(\underline{r}_v) \\ &+ \lim_{q \rightarrow 0} \hat{n}_o(\underline{r}) \times \int_S \underline{G}_{N_s}(\underline{r}_v, \underline{r}') \cdot \underline{J}(\underline{r}') dS' \quad (145) \end{aligned}$$

$$\begin{aligned} \lim_{q \rightarrow 0} \hat{n}_o(\underline{r}) \times \underline{H}_{N_s}(\underline{r}_v) &= \lim_{q \rightarrow 0} \hat{n}_o(\underline{r}) \times \underline{H}_{TN_s}(\underline{r}_v) \\ &+ \lim_{q \rightarrow 0} \hat{n}_o(\underline{r}) \times \int_S \underline{K}_{N_s}(\underline{r}_v, \underline{r}') \cdot \underline{J}(\underline{r}') dS' \quad (146) \end{aligned}$$

Using the continuity of the fields in the region exterior to the scatterer, the boundary condition

$$\hat{n}_O(\underline{r}) \times \underline{E}_{N_S}(\underline{r}) = 0 \quad (147)$$

the previously cited definition,

$$\hat{n}_O(\underline{r}) \times \underline{H}_{N_S}(\underline{r}) = \underline{J}(\underline{r}) \quad (148)$$

and the new definition

$$\hat{n}_O(\underline{r}) \times \underline{H}_{TN_S}(\underline{r}) = \underline{J}_T(\underline{r}) \quad (149)$$

we can write Equations 145 and 146 as

$$-\hat{n}_O(\underline{r}) \times \underline{E}_{TN_S}(\underline{r}) = \underline{I}_{EL} \quad (150)$$

$$\underline{J}(\underline{r}) = \underline{J}_T(\underline{r}) + \underline{I}_{HL} \quad (151)$$

where

$$\underline{I}_{EL} = \lim_{q \rightarrow 0} \hat{n}_O(\underline{r}) \times \int_S \underline{G}_{N_S}(\underline{r}_V, \underline{r}') \cdot \underline{J}(\underline{r}') dS' \quad (152)$$

and

$$\underline{I}_{HL} = \lim_{q \rightarrow 0} \hat{n}_O(\underline{r}) \times \int_S \underline{K}_{N_S}(\underline{r}_V, \underline{r}') \cdot \underline{J}(\underline{r}') dS' \quad (153)$$

The limits in Equations 152 and 153 will be examined by decomposing $\underline{G}_{N_S}(\underline{r}_V, \underline{r}')$ and $\underline{K}_{N_S}(\underline{r}_V, \underline{r}')$ into parts that contain a singularity and the remaining nonsingular parts.

The singular parts will be expressed in such a manner that the limits appearing in Equations 152 and 153 will be seen as being previously evaluated for the derivation of the EFIE and the MFIE in a vacuum environment. To accomplish the desired decomposition, we write the solutions to Equations 40 and 41 for the case $l = \underline{N}_s$ as

$$\underline{E}_{\underline{N}_s}^i(\underline{r}_v, \underline{r}') = \underline{E}_U^i(\underline{r}_v, \underline{r}') + \underline{E}_R^i(\underline{r}_v, \underline{r}') \quad (154)$$

and

$$\underline{H}_{\underline{N}_s}^i(\underline{r}_v, \underline{r}') = \underline{H}_U^i(\underline{r}_v, \underline{r}') + \underline{H}_R^i(\underline{r}_v, \underline{r}') \quad (155)$$

The quantities $\underline{E}_U^i(\underline{r}_v, \underline{r}')$ and $\underline{H}_U^i(\underline{r}_v, \underline{r}')$ not only satisfy Equations 40 and 41 for $\underline{r}_v \in V_{\underline{N}_s}$, but they also satisfy these Equations considering that $V_{\underline{N}_s}$ constituted all of space. They consequently also satisfy the radiation condition at infinity. The subscript notion U is introduced to indicate that all of space uniformly consists of material having parameters $\mu_{\underline{N}_s}$ and $\epsilon_{\underline{N}_s}$. With this understanding of the meaning of \underline{E}_U^i and \underline{H}_U^i , it is possible to present explicit expressions for these quantities. Instead we present explicit expressions for

$$\underline{G}_U(\underline{r}_v, \underline{r}') = \sum_{i=1}^3 \underline{E}_U^i(\underline{r}_v, \underline{r}') \hat{a}_i \quad (156)$$

and

$$\underline{K}_U(\underline{r}_v, \underline{r}') = \sum_{i=1}^3 \underline{H}_U^i(\underline{r}_v, \underline{r}') \hat{a}_i \quad (157)$$

which because of the described meaning of \underline{E}_U^i and \underline{H}_U^i can be rewritten as

$$\underline{G}_U(\underline{r}_v, \underline{r}') = \left(\frac{i\omega\mu_{N_s}}{4\pi} \right) \left(\underline{I} + k_{N_s}^{-2} \nabla_v \nabla_v \right) G_{N_s}(k_{N_s}, R_v) \quad (158)$$

$$\underline{K}_U(\underline{r}_v, \underline{r}') = (4\pi)^{-1} \nabla_v G_{N_s}(k_{N_s}, R_v) \times \underline{I} \quad (159)$$

where

$$G_{N_s}(k_{N_s}, R_v) = R_v^{-1} e^{ik_{N_s} R_v} \quad (160a)$$

$$R_v = |\underline{r}_v - \underline{r}'| \quad (160b)$$

Combining Equations 39, 47, and 154 through 157, we have

$$\underline{G}_{N_s}(\underline{r}_v, \underline{r}') = \underline{G}_U(\underline{r}_v, \underline{r}') + \underline{G}_R(\underline{r}_v, \underline{r}') \quad (161)$$

$$\underline{K}_{N_s}(\underline{r}_v, \underline{r}') = \underline{K}_U(\underline{r}_v, \underline{r}') + \underline{K}_R(\underline{r}_v, \underline{r}') \quad (162)$$

with

$$\underline{G}_R(\underline{r}_v, \underline{r}') = \sum_{i=1}^3 \underline{E}_R^i(\underline{r}_v, \underline{r}') \hat{a}_i \quad (163)$$

$$\underline{K}_R(\underline{r}_v, \underline{r}') = \sum_{i=1}^3 \underline{H}_R^i(\underline{r}_v, \underline{r}') \hat{a}_i \quad (164)$$

where sufficient background has been presented to allow the meaning of $\underline{E}_R^i(\underline{r}_v, \underline{r}')$ and $\underline{H}_R^i(\underline{r}_v, \underline{r}')$ and in turn \underline{G}_R and \underline{K}_R to

receive further elaboration. \underline{E}_R^i and \underline{H}_R^i are solutions to Equations 40 and 41 for $l = N_s$ with the δ function source eliminated. The fields \underline{E}_U^i and \underline{H}_R^i satisfy the inhomogeneous equations, and the purpose of \underline{E}_R^i and \underline{H}_R^i is to cause the fields $\underline{E}_{N_s}^i$ and $\underline{H}_{N_s}^i$ given by Equations 154 and 155 to satisfy the boundary conditions described in Appendix A. From this understanding of the nature of the \underline{G}_R and \underline{K}_R , we can conclude that there are no singularities to be considered in the limit as q approaches zero in terms containing these dyadics. This is expressed explicitly by combining Equations 152, 153, 161, and 162 to obtain

$$\underline{I}_{EL} = \underline{I}_{EU} + \underline{I}_{ER} \quad (165)$$

and

$$\underline{I}_{HL} = \underline{I}_{HU} + \underline{I}_{HR} \quad (166)$$

where

$$\underline{I}_{EU} = \lim_{q \rightarrow 0} \hat{n}_O(\underline{r}) \times \int_S \underline{G}_U(\underline{r}, \underline{r}') \cdot \underline{J}(\underline{r}') dS' \quad (167)$$

$$\underline{I}_{HU} = \lim_{q \rightarrow 0} \hat{n}_O(\underline{r}) \times \int_S \underline{K}_U(\underline{r}, \underline{r}') \cdot \underline{J}(\underline{r}') dS' \quad (168)$$

$$\underline{I}_{ER} = \hat{n}_O(\underline{r}) \times \int_S \underline{G}_R(\underline{r}, \underline{r}') \cdot \underline{J}(\underline{r}') dS' \quad (169)$$

$$\underline{I}_{HR} = \hat{n}_O(\underline{r}) \times \int_S \underline{K}_R(\underline{r}, \underline{r}') \cdot \underline{J}(\underline{r}') dS' \quad (170)$$

The essential behavior of the limits in Equations 167 and 168 is independent of whether k_{Ns}^2 is real or complex. For the case where k_{Ns}^2 is real, these limits have been given considerable attention for the derivation of the free-field EFIE and MFIE. Using the standard results for these limits, we have

$$\underline{I}_{EU} = \hat{n}_O(\underline{r}) \times \left[\left(\underline{I} + k_{Ns}^{-2} \nabla \nabla \cdot \right) \int_S \left(\frac{i\omega\mu_{Ns}}{4\pi} \right) G_{Ns}(k_{Ns}, R_V) \underline{J}(\underline{r}') dS' \right]_{\underline{r}_V = \underline{r}} \quad (171a)$$

or

$$\underline{I}_{EU} = \hat{n}_O(\underline{r}) \times \left[\left(\underline{I} + k_{Ns}^{-2} \nabla \nabla \cdot \right) \int_S \left(\frac{i\omega\mu_{Ns}}{4\pi} \right) G_{Ns}(k_{Ns}, R) \underline{J}(\underline{r}') dS' \right] \quad (171b)$$

and

$$\begin{aligned} \underline{I}_{HU} = \hat{n}_O(\underline{r}) \times & \left\{ \int_S (4\pi)^{-1} \left[\nabla_V G_{Ns}(k_{Ns}, R_V) \times \underline{J}(\underline{r}') \right] dS' \right\} \\ & + \frac{\Omega}{4\pi} \underline{J}(\underline{r}) \end{aligned} \quad \underline{r}_V = \underline{r} \quad (172a)$$

or

$$\begin{aligned} \underline{I}_{HU} = \hat{n}_O(\underline{r}) \times & \int_S (4\pi)^{-1} \left[\nabla G_{Ns}(k_{Ns}, R) \times \underline{J}(\underline{r}') \right] dS' \\ & \times \frac{\Omega}{4\pi} \underline{J}(\underline{r}) \end{aligned} \quad (172b)$$

where Ω is the solid angle subtended by the surface at \underline{r} . The usual expressions for the limits are given in Equations 171b and 172b; however, the real meaning is better understood by referring to expressions 171a and 172a. It should be noted that none of the integrals in Equations 171 and 172 are principal-value integrals. Finally, we refer to Reference 8 for alternate expressions for Equation 171.

Combining Equations 150, 161, 165, 169, and 171, we have for the EFIE

$$\begin{aligned} -\hat{n}_O(\underline{r}) \times \underline{E}_{TN_S}(\underline{r}) &= \hat{n}_O(\underline{r}) \times \left[\left(\underline{I} + k_{N_S}^{-2} \nabla \nabla \cdot \right) \int_S \left(\frac{i\omega\mu_N \underline{s}}{4\pi} \right) G_{N_S}(k_{N_S}, R) \underline{J}(\underline{r}') dS' \right] \\ &+ \hat{n}_O(\underline{r}) \times \int_S \left[\underline{G}_{N_S}(\underline{r}, \underline{r}') - \underline{G}_U(\underline{r}, \underline{r}') \right] \cdot \underline{J}(\underline{r}') dS' \end{aligned} \quad (173)$$

Combining Equations 151, 162, 166, 170, and 172, we have for the MFIE

$$\begin{aligned} \left(1 - \frac{\Omega}{4\pi} \right) \underline{J}(\underline{r}) &= \underline{J}_T(\underline{r}) + \hat{n}_O(\underline{r}) \times \int_S (4\pi)^{-1} \left[\nabla G_{N_S}(k_{N_S}, R) \right] \times \underline{J}(\underline{r}') dS' \\ &+ \hat{n}_O(\underline{r}) \times \int_S \left[\underline{K}_{N_S}(\underline{r}, \underline{r}') - \underline{K}_U(\underline{r}, \underline{r}') \right] \cdot \underline{J}(\underline{r}') dS' \end{aligned} \quad (174)$$

There are two important points to note about the representations given by these equations. The first is that this decomposition is not just formal as can be seen by observing Equations 92, 93, 114, and 115 for the two-layered medium. The second is that the numerical treatment of these equations can be facilitated by using these representations. For the MFIE numerical

solution of the two-layered scattering problem, we use this decomposition and pay particular attention to the treatment of the integrable singularity that exists in the first integral appearing in Equation 174.

VI. EXPLICIT SYMMETRY ARGUMENTS FOR THE TWO LAYERED MFIE

The actual surface that was numerically treated had a plane of symmetry perpendicular to the ground plane, and this allowed us to reduce the computer time to solve the problem numerically. For the purposes of illustration, we will choose our coordinate system so that the symmetry plane of the body corresponds to the plane $x = 0$; however, the final results will appear in a form that is invariant to this coordinate choice. First we write Equation 174 as specialized to the two-layered problem discussed in Section III as

$$f(\Omega)\underline{J}(\underline{r}) = \underline{J}_T(\underline{r}) + \int_S \underline{D}(\underline{r}, \underline{r}') \cdot \underline{J}(\underline{r}') dS' \quad (175)$$

where

$$f(\Omega) = 1 - \frac{\Omega}{4\pi} \quad (176)$$

and

$$\underline{D}(\underline{r}, \underline{r}') = \hat{n}_O(\underline{r}) \times \underline{K}_2(\underline{r}, \underline{r}') \quad (177)$$

and alternate explicit representations of $\underline{K}_2(\underline{r}, \underline{r}')$ are obtained by combining Equations 93, 95, 106 through 109 and either 104 and 105 or 115 depending on our choice of representation for the $\underline{K}_O(\underline{r}, \underline{r}')$ portion of $\underline{K}_2(\underline{r}, \underline{r}')$. For the choice of Equation 115 to represent $\underline{K}_O(\underline{r}, \underline{r}')$, all necessary symmetry arguments have been presented in Reference 1, and we could make use of those arguments. Instead, it provides little more effort to consider Equations 104 and 105 for the representation and thus presents a self-contained derivation.

We now write Equation 175 as

$$\begin{aligned} f(\Omega) \underline{J}(\underline{r}_+) &= \underline{J}_T(\underline{r}_+) + \int_{S_+} \underline{D}(\underline{r}_+, \underline{r}') \cdot \underline{J}(\underline{r}') dS' \\ &+ \int_{S_-} \underline{D}(\underline{r}_+, \underline{r}') \cdot \underline{J}(\underline{r}') dS' \end{aligned} \quad (178)$$

and

$$\begin{aligned} f(\Omega) \underline{J}(\underline{r}_-) &= \underline{J}_T(\underline{r}_-) + \int_{S_+} \underline{D}(\underline{r}_-, \underline{r}') \cdot \underline{J}(\underline{r}') dS' \\ &+ \int_{S_-} \underline{D}(\underline{r}_-, \underline{r}') \cdot \underline{J}(\underline{r}') dS' \end{aligned} \quad (179)$$

where \underline{r}_+ and \underline{r}'_+ describe points having positive x -coordinates while \underline{r}_- and \underline{r}'_- describe points having negative x -coordinates. The integration over S_+ is over the surface having positive x coordinates, and the integration over S_- is over the surface having negative x -coordinates. The explicit relationship between symmetric points is

$$\underline{r}_- = \underline{R}_x \cdot \underline{r}_+ \quad (180a)$$

$$\underline{r}'_- = \underline{R}_x \cdot \underline{r}'_+ \quad (180b)$$

where

$$\underline{R}_x = \underline{I} - 2\hat{a}_x \hat{a}_x \quad (181)$$

We now rewrite Equations 178 and 179 after operating on both sides of Equation 179 with \underline{R}_x to obtain

$$\begin{aligned} f(\Omega) \underline{J}^+(\underline{r}_+) &= \underline{J}_T^+(\underline{r}_+) + \int_{S_+} \underline{D}_{++}(\underline{r}_+, \underline{r}'_+) \cdot \underline{J}^+(\underline{r}'_+) dS' \\ &+ \int_{S_+} \underline{D}_{+-}(\underline{r}_+, \underline{r}'_+) \cdot \underline{J}^-(\underline{r}'_+) dS' \end{aligned} \quad (182)$$

$$\begin{aligned} f(\Omega) \underline{J}^-(\underline{r}_+) &= \underline{J}_T^-(\underline{r}_+) + \int_{S_+} \underline{D}_{-+}(\underline{r}_+, \underline{r}'_+) \cdot \underline{J}^+(\underline{r}'_+) dS' \\ &+ \int_{S_+} \underline{D}_{--}(\underline{r}_+, \underline{r}'_+) \cdot \underline{J}^-(\underline{r}'_+) dS' \end{aligned} \quad (183)$$

where

$$\underline{J}^+(\underline{r}_+) = \underline{J}(\underline{r}_+) \quad (184a)$$

$$\underline{J}^+(\underline{r}'_+) = \underline{J}(\underline{r}'_+) \quad (184b)$$

$$\underline{J}_T^+(\underline{r}_+) = \underline{J}_T(\underline{r}_+) \quad (185)$$

$$\underline{J}^-(\underline{r}_+) = \underline{R}_x \cdot \underline{J}(\underline{R}_x \cdot \underline{r}_+) \quad (186a)$$

$$\underline{J}^-(\underline{r}'_+) = \underline{R}_x \cdot \underline{J}(\underline{R}_x \cdot \underline{r}'_+) \quad (186b)$$

$$\underline{J}_T^-(\underline{r}_+) = \underline{R}_x \cdot \underline{J}_T(\underline{R}_x \cdot \underline{r}_+) \quad (187)$$

$$\underline{D}_{++}(\underline{r}_+, \underline{r}'_+) = \underline{D}(\underline{r}_+, \underline{r}'_+) \quad (188)$$

$$\underline{D}_{+-}(\underline{r}_+, \underline{r}'_+) = \underline{D}(\underline{r}_+, \underline{R}_x \cdot \underline{r}'_+) \cdot \underline{R}_x \quad (189)$$

$$\underline{D}_{-+}(\underline{r}_+, \underline{r}'_+) = \underline{R}_x \cdot \underline{D}(\underline{R}_x \cdot \underline{r}_+, \underline{r}'_+) \quad (190)$$

$$\underline{D}_{--}(\underline{r}_+, \underline{r}'_+) = \underline{R}_x \cdot \underline{D}(\underline{R}_x \cdot \underline{r}_+, \underline{R}_x \cdot \underline{r}'_+) \cdot \underline{R}_x \quad (191)$$

and in order to obtain Equations 182 and 183 we substituted the unit dyadic, \underline{I} , expressed as

$$\underline{I} = \underline{R}_x \cdot \underline{R}_x \quad (192)$$

to obtain the relationships

$$\underline{D}(\underline{r}_+, \underline{r}'_+) \cdot \underline{J}(\underline{r}'_-) = \left[\underline{D}(\underline{r}_+, \underline{r}'_+) \cdot \underline{R}_x \right] \cdot \left[\underline{R}_x \cdot \underline{J}(\underline{r}'_-) \right] \quad (193)$$

and

$$\underline{D}(\underline{r}_-, \underline{r}'_-) \cdot \underline{J}(\underline{r}'_-) = \left[\underline{D}(\underline{r}_-, \underline{r}'_-) \cdot \underline{R}_x \right] \cdot \left[\underline{R}_x \cdot \underline{J}(\underline{r}'_-) \right] \quad (194)$$

which in turn are utilized in those equations. If the following relationships are true,

$$\underline{D}_{++}(\underline{r}_+, \underline{r}'_+) = \underline{D}_{--}(\underline{r}_+, \underline{r}'_+) \equiv \underline{A}(\underline{r}_+, \underline{r}'_+) \quad (195)$$

and

$$\underline{D}_{+-}(\underline{r}_+, \underline{r}'_+) = \underline{D}_{-+}(\underline{r}_+, \underline{r}'_+) \equiv \underline{B}(\underline{r}_+, \underline{r}'_+) \quad (196)$$

then by first adding and then subtracting Equations 182 and 183, we obtain

$$f(\Omega) \underline{J}_S(\underline{r}_+) = \underline{J}_{TS}(\underline{r}_+) + \int_{S_+} \underline{D}_S(\underline{r}_+, \underline{r}'_+) \cdot \underline{J}_S(\underline{r}'_+) dS' \quad (197)$$

and

$$f(\Omega) \underline{J}_A(\underline{r}_+) = \underline{J}_{TA}(\underline{r}_+) + \int_{S_+} \underline{D}(\underline{r}_+, \underline{r}'_+) \cdot \underline{J}_A(\underline{r}'_+) dS' \quad (198)$$

where

$$\underline{J}_S(\underline{r}_+) = \frac{1}{2} \left[\underline{J}^+(\underline{r}_+) + \underline{J}^-(\underline{r}_+) \right] \quad (199a)$$

$$\underline{J}_S(\underline{r}'_+) = \frac{1}{2} \left[\underline{J}^+(\underline{r}'_+) + \underline{J}^-(\underline{r}'_+) \right] \quad (199b)$$

$$\underline{J}_{TS}(\underline{r}'_+) = \frac{1}{2} \left[\underline{J}_T^+(\underline{r}_+) + \underline{J}_T^-(\underline{r}_+) \right] \quad (200)$$

$$\underline{J}_A(\underline{r}_+) = \frac{1}{2} \left[\underline{J}^+(\underline{r}_+) - \underline{J}^-(\underline{r}_+) \right] \quad (201)$$

$$\underline{J}_A(\underline{r}'_+) = \frac{1}{2} \left[\underline{J}^+(\underline{r}'_+) - \underline{J}^-(\underline{r}'_+) \right] \quad (202)$$

$$\underline{J}_{TA}(\underline{r}_+) = \frac{1}{2} \left[\underline{J}_T^+(\underline{r}_+) - \underline{J}_T^-(\underline{r}_+) \right] \quad (203)$$

$$\underline{D}_S(\underline{r}_+, \underline{r}'_+) = \underline{A}(\underline{r}_+, \underline{r}'_+) + \underline{B}(\underline{r}_+, \underline{r}'_+) \quad (204)$$

$$\underline{D}_A(\underline{r}_+, \underline{r}'_+) = \underline{A}(\underline{r}_+, \underline{r}'_+) - \underline{B}(\underline{r}_+, \underline{r}'_+) \quad (205)$$

and the advantage of Equations 197 and 198 over 175 will be explained. Following that explanation, a proof that Equations 195 and 196 are true will conclude this section.

The essential property that the set of Equations 197 and 198 have is that only half of the symmetric surface requires numerical treatment. The resulting matrix that gets generated for each of the Equations 197 and 198 is half as large as the matrix that would get generated by the straightforward numerical treatment of Equation 175. Because matrix inversion time is proportional to the cube of the matrix size, there is a factor of four savings in inverting two matrices that are half the size of a larger matrix since

$$2\left(\frac{N}{2}\right)^3 = \frac{1}{4} N^3$$

Regarding the matrix generation time, there is a forced savings caused by seeking the relationships expressed by Equations 195 and 196. The reason there is a forced savings is that the straightforward treatment would effectively require that each matrix element be viewed as receiving a contribution from $\underline{D}_{++}, \underline{D}_{--}, \underline{D}_{+-},$ and \underline{D}_{-+} , while Equations 195 and 196 show that there are only two independent contributors. Returning to Equations 197 and 198, we numerically solve for \underline{J}_S and \underline{J}_A which in turn yield the desired physical quantities $\underline{J}(\underline{r}_+)$ and $\underline{J}(\underline{r}_-)$ by employing the relationships

$$\underline{J}(\underline{r}_+) = \underline{J}_S(\underline{r}_+) + \underline{J}_A(\underline{r}_+) \quad (206)$$

$$\underline{J}(\underline{r}_-) = \underline{R}_x \cdot \left[\underline{J}_S(\underline{r}_+) - \underline{J}_A(\underline{r}_+) \right] \quad (207)$$

Returning to the proof of the validity of Equations 195 and 196, we identify the explicit meaning of these quantities as

$$\underline{D}_{++}(\underline{r}_+, \underline{r}'_+) = \hat{n}_O(\underline{r}_+) \times \underline{K}(\underline{r}_+, \underline{r}'_+) \quad (208)$$

$$\underline{D}_{--}(\underline{r}_+, \underline{r}'_+) = \underline{R}_x \cdot \left[\hat{n}_O(\underline{r}_-) \times \underline{K}(\underline{r}_+, \underline{r}'_+) \right] \cdot \underline{R}_x \quad (209)$$

$$\underline{D}_{+-}(\underline{r}_+, \underline{r}'_+) = \left[\hat{n}_O(\underline{r}_+) \times \underline{K}(\underline{r}_+, \underline{r}'_+) \right] \cdot \underline{R}_x \quad (210)$$

$$\underline{D}_{-+}(\underline{r}_+, \underline{r}'_+) = \underline{R}_x \cdot \left[(\hat{n}_O(\underline{r}_-) \times \underline{K}(\underline{r}_-, \underline{r}'_+)) \right] \quad (211)$$

and the definition of $\underline{K}(\underline{r}, \underline{r}')$ is given by combining Equations 93, 95, and 104 through 109. For the purposes of this section, we write the essential form

$$\begin{aligned} \underline{K}(\underline{r}, \underline{r}') &= K_{\rho\phi}(\underline{r}, \underline{r}') \hat{a}_{\rho_D}(\underline{r}, \underline{r}') \hat{a}_{\phi_D}(\underline{r}, \underline{r}') \\ &+ K_{\rho\phi}(\underline{r}, \underline{r}') \hat{a}_{\phi_D}(\underline{r}, \underline{r}') \hat{a}_{\rho_D}(\underline{r}, \underline{r}') \\ &+ K_{z\phi}(\underline{r}, \underline{r}') \hat{a}_z \hat{a}_{\phi_D}(\underline{r}, \underline{r}') \\ &+ K_{\phi z}(\underline{r}, \underline{r}') \hat{a}_{\phi_D}(\underline{r}, \underline{r}') \hat{a}_z \end{aligned} \quad (212)$$

with the essential property extracted from those equations that

$$K_{\alpha\beta}(\underline{r}_+, \underline{r}'_+) = K_{\alpha\beta}(\underline{r}_-, \underline{r}'_-) \quad (213)$$

and

$$K_{\alpha\beta}(\underline{r}_+, \underline{r}'_-) = K_{\alpha\beta}(\underline{r}_-, \underline{r}'_+) \quad (214)$$

with α and β taking on the notation $\rho, \phi,$ and z to generate the four terms appearing in Equation 212. Equations 213 and 214 follow by noting that according to Equations 105 through 109

$$K_{\alpha\beta}(\underline{r}, \underline{r}') = K_{\alpha\beta}(|\underline{r} - \underline{r}'|) + K_{s\alpha\beta}(|\underline{\rho} - \underline{\rho}'|, z + z') \quad (215)$$

The more difficult aspect of proving Equations 195 and 196 is related to the dyadic character of these equations. To complete this aspect of the proof, we will introduce the following dyadic identities which will later be proved.

$$\underline{R}_x \cdot (\underline{A} \times \underline{B}) = -(\underline{R}_x \cdot \underline{A}) \times (\underline{R}_x \cdot \underline{B}) \quad (216)$$

$$\underline{R}_x \cdot (\underline{A} \times \underline{C}) = -(\underline{R}_x \cdot \underline{A}) \times (\underline{R}_y \cdot \underline{C}) \quad (217)$$

$$(\underline{A} \times \underline{C}) \cdot \underline{R}_x = \underline{A} \times (\underline{C} \cdot \underline{R}_x) \quad (218)$$

Using these equations as well as Equations 212, 213, and 214, we can write Equations 208 through 211 as

$$\begin{aligned}
\underline{D}_{++}(\underline{r}_+, \underline{r}'_+) &= \hat{n}_O(\underline{r}_+) \times \left\{ K_{\rho\phi}(\underline{r}_+, \underline{r}'_+) \hat{a}_{\rho_D}(\underline{r}_+, \underline{r}'_+) \hat{a}_{\phi_D}(\underline{r}_+, \underline{r}'_+) \right. \\
&+ K_{\phi\rho}(\underline{r}_+, \underline{r}'_+) \hat{a}_{\phi_D}(\underline{r}_+, \underline{r}'_+) \hat{a}_{\rho_D}(\underline{r}_+, \underline{r}'_+) \\
&+ K_{z\phi}(\underline{r}_+, \underline{r}'_+) \hat{a}_z \hat{a}_{\phi_D}(\underline{r}_+, \underline{r}'_+) \\
&\left. + K_{\phi z}(\underline{r}_+, \underline{r}'_+) \hat{a}_{\phi_D}(\underline{r}_+, \underline{r}'_+) \hat{a}_z \right\} \quad (219)
\end{aligned}$$

$$\begin{aligned}
\underline{D}_{--}(\underline{r}_+, \underline{r}'_+) &= -\underline{R}_x \cdot \hat{n}_O(\underline{r}_-) \times \left\{ K_{\rho\phi}(\underline{r}_+, \underline{r}'_+) \left[\underline{R}_x \cdot \hat{a}_{\rho_D}(\underline{r}_-, \underline{r}'_-) \right] \left[\hat{a}_{\rho_D}(\underline{r}_-, \underline{r}'_-) \cdot \underline{R}_x \right] \right. \\
&+ K_{\phi\rho}(\underline{r}_+, \underline{r}'_+) \left[\underline{R}_x \cdot \hat{a}_{\phi_D}(\underline{r}_-, \underline{r}'_-) \right] \left[\hat{a}_{\rho_D}(\underline{r}_-, \underline{r}'_-) \cdot \underline{R}_x \right] \\
&+ K_{z\phi}(\underline{r}_+, \underline{r}'_+) \left(\underline{R}_x \cdot \hat{a}_z \right) \left[\hat{a}_{\phi_D}(\underline{r}_-, \underline{r}'_-) \cdot \underline{R}_x \right] \\
&\left. + K_{\phi z}(\underline{r}_+, \underline{r}'_+) \left[\underline{R}_x \cdot \hat{a}_{\phi_D}(\underline{r}_-, \underline{r}'_-) \right] \left(\hat{a}_z \cdot \underline{R}_x \right) \right\} \quad (220)
\end{aligned}$$

$$\begin{aligned}
\underline{D}_{+-}(\underline{r}_+, \underline{r}'_+) &= \hat{n}_O(\underline{r}_+) \times \left\{ K_{\rho\phi}(\underline{r}_+, \underline{r}'_+) \hat{a}_{\rho_D}(\underline{r}_+, \underline{r}'_+) \left[\hat{a}_{\phi_D}(\underline{r}_+, \underline{r}'_+) \cdot \underline{R}_x \right] \right. \\
&+ K_{\phi\rho}(\underline{r}_+, \underline{r}'_+) \hat{a}_{\phi_D}(\underline{r}_+, \underline{r}'_+) \left[\hat{a}_{\rho_D}(\underline{r}_+, \underline{r}'_+) \cdot \underline{R}_x \right] \\
&+ K_{z\phi}(\underline{r}_+, \underline{r}'_+) \hat{a}_z \left[\hat{a}_{\phi_D}(\underline{r}_+, \underline{r}'_+) \cdot \underline{R}_x \right] \\
&\left. + K_{\phi z}(\underline{r}_+, \underline{r}'_+) \hat{a}_{\phi_D}(\underline{r}_+, \underline{r}'_+) \left(\hat{a}_z \cdot \underline{R}_x \right) \right\} \quad (221)
\end{aligned}$$

$$\begin{aligned}
D_{-+}(\underline{r}_+, \underline{r}_+) = & - \left[\underline{R}_x \cdot \hat{n}_0(\underline{r}_-) \right] \times \left\{ K_{\rho\phi}(\underline{r}_+, \underline{r}_-) \left[\underline{R}_x \cdot \hat{a}_{\rho_D}(\underline{r}_-, \underline{r}_+) \right] \hat{a}_{\phi_D}(\underline{r}_-, \underline{r}_+) \right. \\
& + K_{\phi\rho}(\underline{r}_+, \underline{r}_-) \left[\underline{R}_x \cdot \hat{a}_{\phi_D}(\underline{r}_-, \underline{r}_+) \right] \hat{a}_{\rho_D}(\underline{r}_-, \underline{r}_+) \\
& + K_{z\phi}(\underline{r}_+, \underline{r}_-) (\underline{R}_x \cdot \hat{a}_z) \hat{a}_{\phi_D}(\underline{r}_-, \underline{r}_+) \\
& \left. + K_{\phi z}(\underline{r}_+, \underline{r}_-) \left[\underline{R}_x \cdot \hat{a}_{\phi_D}(\underline{r}_-, \underline{r}_+) \right] \hat{a}_z \right\} \quad (222)
\end{aligned}$$

The equations, which when substituted into Equations 219 through 222 lead to the desired results, will be presented. First we present the following representations for \hat{a}_{ρ_D} where x and x' are positive

$$\hat{a}_{\rho_D}(\underline{r}_+, \underline{r}_+) = \frac{(x-x')\hat{a}_x + (y-y')\hat{a}_y}{\rho_-} \quad (223)$$

$$\hat{a}_{\rho_D}(\underline{r}_-, \underline{r}_-) = \frac{-(x-x')\hat{a}_x + (y-y')\hat{a}_y}{\rho_-} \quad (224)$$

$$\hat{a}_{\rho_D}(\underline{r}_+, \underline{r}_-) = \frac{(x+x')\hat{a}_x + (y-y')\hat{a}_y}{\rho_+} \quad (225)$$

$$\hat{a}_{\rho_D}(\underline{r}_-, \underline{r}_+) = \frac{-(x+x')\hat{a}_x + (y-y')\hat{a}_y}{\rho_+} \quad (226)$$

$$\rho_- = \left[(x-x')^2 + (y-y')^2 \right]^{1/2} \quad (227)$$

$$\rho_+ = \left[(x+x')^2 + (y-y')^2 \right]^{1/2} \quad (228)$$

By simply applying the indicated operations on the preceding equations, it follows that

$$\underline{R}_x \cdot \hat{a}_{\rho_D}(\underline{r}_-, \underline{r}') = \hat{a}_{\rho_D}(\underline{r}_-, \underline{r}') \cdot \underline{R}_x = \hat{a}_{\rho_D}(\underline{r}_+, \underline{r}') \quad (229)$$

$$\hat{a}_{\rho_D}(\underline{r}_+, \underline{r}') \cdot \underline{R}_x = \hat{a}_{\rho_D}(\underline{r}_-, \underline{r}') \quad (230)$$

$$\underline{R}_x \cdot \hat{a}_{\rho_D}(\underline{r}_-, \underline{r}') = \hat{a}_{\rho_D}(\underline{r}_+, \underline{r}') \quad (231)$$

Next using the definition

$$\hat{a}_{\phi_D}(\underline{r}, \underline{r}') = \hat{a}_z \times \hat{a}_{\rho_D}(\underline{r}, \underline{r}')$$

as well as Equation 216 and the fact that

$$\underline{R}_x \cdot \hat{a}_z = \hat{a}_z \cdot \underline{R}_x = \hat{a}_z \quad (232)$$

we find that

$$\underline{R}_x \cdot \hat{a}_{\phi_D}(\underline{r}_-, \underline{r}') = \hat{a}_{\phi_D}(\underline{r}_-, \underline{r}') \cdot \underline{R}_x = -\hat{a}_{\phi_D}(\underline{r}_+, \underline{r}') \quad (233)$$

$$\hat{a}_{\phi_D}(\underline{r}_+, \underline{r}') \cdot \underline{R}_x = -\hat{a}_{\phi_D}(\underline{r}_-, \underline{r}') \quad (234)$$

$$\underline{R}_x \cdot \hat{a}_{\phi_D}(\underline{r}_-, \underline{r}') = -\hat{a}_{\phi_D}(\underline{r}_+, \underline{r}') \quad (235)$$

The final relationship needed follows from the basic symmetry of the body, and it is

$$\underline{R}_x \cdot \hat{n}_O(\underline{r}_-) = \hat{n}_O(\underline{r}_+) \quad (236)$$

Substituting Equations 229, 230, 231, as well as 232 through 236 into Equations 219 through 222 yields the desired results, i.e., Equations 195 and 196.

This section is concluded by presenting the derivation of Equations 216, 217, and 218 as promised prior to the use of these equations. First, we decompose general vectors, \underline{A} and \underline{B} , as follows

$$\underline{A} = \underline{A}_T + A_x \hat{a}_x \quad (237)$$

and

$$\underline{B} = \underline{B}_T + B_x \hat{a}_x \quad (238)$$

where the subscript T indicates a direction orthogonal to \hat{a}_x . We now form the cross product

$$\underline{A} \times \underline{B} = \underline{A}_T \times \underline{B}_T + A_x \hat{a}_x \times \underline{B}_T + \underline{A}_T \times B_x \hat{a}_x \quad (239)$$

and note that the first term on the right-hand side of Equation 239 is directed strictly along the \hat{a}_x direction while the second and third terms have no \hat{a}_x directed components. Using this observation, it follows that

$$\underline{R}_x \cdot (\underline{A} \times \underline{B}) = -\underline{A}_T \times \underline{B}_T + A_x \hat{a}_x \times \underline{B}_T + \underline{A}_T \times B_x \hat{a}_x \quad (240)$$

Operating on the expressions given in Equations 237 and 238 and then forming the cross product, it follows that

$$(\underline{\underline{R}}_x \cdot \underline{A}) \times (\underline{\underline{R}}_x \cdot \underline{B}) = \underline{A}_T \times \underline{B}_T - \underline{A}_x \hat{a}_x \times \underline{B}_T - \underline{A}_T \times \underline{B}_x \hat{a}_x \quad (241)$$

Multiplying this equation by minus one and substituting the result into Equation 240 yields the desired result, i.e., Equation 216. Next we express a general dyadic $\underline{\underline{C}}$ as

$$\underline{\underline{C}} = \sum_{i=1}^3 \underline{E}_i \underline{F}_i \quad (242)$$

so that we can write

$$\underline{A} \times \underline{\underline{C}} = \sum_{i=1}^3 (\underline{A} \times \underline{E}_i) \underline{F}_i \quad (243)$$

Operating on this equation to the left with $\underline{\underline{R}}_x$ yields

$$\underline{\underline{R}}_x \cdot (\underline{A} \times \underline{\underline{C}}) = \sum_{i=1}^3 \left[\underline{\underline{R}}_x \cdot (\underline{A} \times \underline{E}_i) \right] \underline{F}_i \quad (244)$$

any by utilizing Equation 216, we obtain

$$\begin{aligned} \underline{\underline{R}}_x \cdot (\underline{A} \times \underline{\underline{C}}) &= \sum_{i=1}^3 -(\underline{\underline{R}}_x \cdot \underline{A}) \times (\underline{\underline{R}}_x \cdot \underline{E}_i) \underline{F}_i \\ &= -(\underline{\underline{R}}_x \cdot \underline{A}) \times \underline{\underline{R}}_x \cdot \sum_{i=1}^3 \underline{E}_i \underline{F}_i \end{aligned} \quad (245)$$

which becomes Equation 217 after resubstituting Equation 242.
Writing

$$\begin{aligned}
 (\underline{A} \times \underline{C}) \cdot \underline{R}_x &= \left[\underline{A} \times \left(\sum_{i=1}^3 \underline{E}_i \underline{F}_i \right) \right] \cdot \underline{R}_x \\
 &= \underline{A} \times \sum_{i=1}^3 \underline{E}_i (\underline{F}_i \cdot \underline{R}_x) \\
 &= \underline{A} \times (\underline{C} \cdot \underline{R}_x)
 \end{aligned} \tag{246}$$

completes the derivation of Equations 216, 217, and 218.

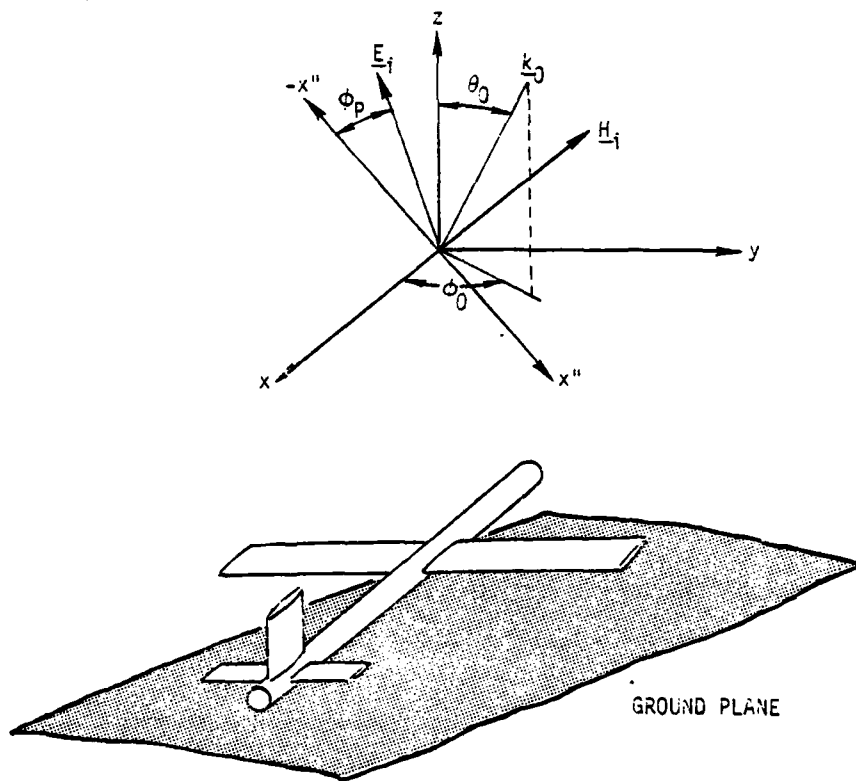
VII. CODE TESTING

1. INTRODUCTION

The incorporation of a lossy half space into our MFIE code (NEC-2A), described in Reference 1, was complicated by the absence of data related to the model depicted in Figure 4 that could be used to quantify the accuracy of the added capability. Special tests had to be devised to detect the presence of coding errors.

In this section we describe the steps taken to establish confidence in the added code. We first summarize these steps and then, for the interested reader, discuss the detailed considerations. At the end of this section we discuss some of the accuracy considerations for the numerical procedures.

- As can be seen from Equations 62 through 73, the computer code would require the derivatives of U_{22} , V_{22} and W_{22} . Although we were unable to obtain tables of necessary quantities, we did find tables for U_{22} and V_{22} (Equations 89 and 90). We therefore developed computer codes for calculating these integrals and validated these codes over the range of the tables. We then developed the subroutines that would be used to calculate the U_{22} , V_{22} and W_{22} derivative terms. The U_{22} and V_{22} derivatives were verified by direct comparison to the numerical derivatives of the terms previously calculated. The W_{22} derivatives were validated indirectly through relationships between U_{22} , V_{22} and W_{22} .
- New coding was required to incorporate the new terms into the matrix of influence coefficients. By examining the limit of a perfectly conducting half-space, we were able to verify that the new code properly communicated with the other modules of the computer code.



$$\begin{aligned}
 \hat{k} &= -\cos\phi_0 \sin\theta_0 \hat{e}_x - \sin\phi_0 \sin\theta_0 \hat{e}_y - \cos\theta_0 \hat{e}_z \\
 \hat{E} &= (-\cos\phi_0 \cos\phi_p \cos\theta_0 - \sin\phi_p \sin\phi_0) \hat{e}_x \\
 &\quad + (-\sin\phi_0 \cos\phi_p \cos\theta_0 + \sin\phi_p \cos\phi_0) \hat{e}_y \\
 &\quad + \cos\phi_p \sin\theta_0 \hat{e}_z \\
 \hat{H} &= (\sin\phi_p \cos\phi_0 \cos\theta_0 - \cos\phi_p \sin\phi_0) \hat{e}_x \\
 &\quad + (\sin\phi_p \sin\phi_0 \cos\theta_0 + \cos\phi_p \cos\phi_0) \hat{e}_y \\
 &\quad - \sin\phi_p \sin\theta_0 \hat{e}_z
 \end{aligned}$$

Figure 4. Description of the incident plane electromagnetic wave. Axis x'' is the intersection of the z, \underline{k} plane and a plane perpendicular to \underline{k} at the origin.

- In the limit of the half-space having the dielectric properties of free-space, the code should produce its free-space answers. In this manner we were able to validate the relative sign of the additional terms.
- The Lawrence Livermore Laboratory Nuclear Electromagnetics Code (NEC-(1,2)A) can calculate the bulk current for a special case of the situation considered in this report. By integrating the longitudinal current densities of our own predictions, we showed that our results agreed to within five percent of those produced by the NEC-(1,2)A code for our test case.
- Our final test was a comparison to experimental data obtained at the University of Michigan for a situation that could presumably be modelled by our code. We made comparisons for a cylinder in free space, a cylinder above a perfectly conducting ground plane, and a cylinder above a planar lossy surface. Qualitatively, there is agreement for all three situations; quantitatively, there are explainable discrepancies at resonances for the perfectly conducting cases, but the discrepancies for the cases involving a planar lossy surface are larger than expected. It is possible that the quantitative discrepancies for the lossy planar surface are due to differences between the numerical model and the physical situation in which the lossy half-space was an inadequate representation of the lossy material.

We will now amplify the above summary for those readers who are interested.

2. VERIFICATION OF BASIC QUANTITIES

As explained in the beginning of this section, we were unable to obtain tables for the quantities $\frac{\partial U_{22}}{\partial \rho_D}$, $\frac{\partial U_{22}}{\partial z}$, $\frac{\partial V_{22}}{\partial \rho_D}$, $\frac{\partial W_{22}}{\partial \rho_D}$ and $\frac{\partial W_{22}}{\partial \rho_D^2}$. Instead, we developed subroutines to compute

U_{22} and V_{22} and verified their accuracy through comparison to published tables (Reference 9). Having verified the accuracy of these subroutines we proceeded to calculate the partial derivatives of U_{22} and V_{22} by applying finite difference techniques to the results provided by the above-mentioned subroutines. These finite difference estimates of the partial derivatives were in turn used as our reference for validating the subroutines used in the larger computer code.

It was our judgment that the above partial derivatives could be more economically and more stably calculated if they were analytically included inside the integrals defining the required terms. We therefore coded these quantities as follows:

$$\frac{\partial U_{22}}{\partial \rho_D} = -2 \int_0^\infty d\lambda e^{-\gamma_2(z+z')} J_1(\lambda \rho_D) \frac{\lambda^2}{\gamma_1 + \gamma_2} \quad (247)$$

$$\frac{\partial U_{22}}{\partial z} = -2 \int_0^\infty d\lambda e^{-\gamma_2(z+z')} J_0(\lambda \rho_D) \frac{\gamma_2 \lambda}{\gamma_1 + \gamma_2} \quad (248)$$

$$\frac{\partial V_{22}}{\partial \rho_D} = -2 \int_0^\infty d\lambda e^{-\gamma_2(z+z')} J_1(\lambda \rho_D) \frac{\lambda^2}{k^2 \gamma_2 + k_0^2 \gamma_1} \quad (249)$$

$$\frac{\partial W_{22}}{\partial \rho_D} = -2 \int_0^\infty d\lambda e^{-\gamma_2(z+z')} J_1(\lambda \rho_D) \frac{(\gamma_2 - \gamma_1) \lambda^2}{k^2 \gamma_2 + k_0^2 \gamma_1} \quad (250)$$

$$\frac{\partial^2 W_{22}}{\partial \rho_D^2} = -2 \int_0^\infty d\lambda e^{-\gamma_2(z+z')} \left(J_0(\lambda \rho_D) - \frac{J_1(\lambda \rho_D)}{\lambda \rho_D} \right) \frac{(\gamma_2 - \gamma_1) \lambda^3}{k^2 \gamma_2 + k_0^2 \gamma_1} \quad (251)$$

where ρ_D , z , and z' are defined as in Equations 54, 55 and 56

k_0 = Wave number of the incident wave in free space.

k = Complex wave number of the wave transmitted through the lossy half-space; k has a positive imaginary part.

The accuracy of $\frac{\partial U_{22}}{\partial \rho_D}$, $\frac{\partial U_{22}}{\partial z}$ and $\frac{\partial V_{22}}{\partial \rho_D}$ were checked by comparison to the previously established finite difference results. $\frac{\partial W_{22}}{\partial \rho_D}$ and $\frac{\partial^2 W_{22}}{\partial \rho_D^2}$ could not be checked by these means.

We indirectly validated the quantities by showing that they satisfied

$$\frac{\partial^2 W_{22}}{\partial \rho_D^2} + \frac{1}{\rho_D} \frac{\partial W_{22}}{\partial \rho_D} = -2 \frac{\partial G_{21}}{\partial z} + k^2 \frac{\partial V_{22}}{\partial z} + \frac{\partial U_{22}}{\partial z} \quad (252)$$

3. USAGE OF THE LOSSY HALF-SPACE TERMS

The matrix is computed as the sum of three matrices: a free-space matrix, a matrix due to the presence of a perfectly conducting ground plane, and a correction matrix to account for the discrepancy between a perfectly conducting half-space and a lossy half-space. This decomposition is described in Reference 1.

The form of the free-space operator, consistent with the actual programming, is

$$\frac{\hat{n}(\underline{r})}{4\pi} \times \int (\underline{r}-\underline{r}') \times \underline{\underline{I}} \frac{e^{ik|\underline{r}-\underline{r}'|}}{|\underline{r}-\underline{r}'|^3} (ik|\underline{r}-\underline{r}'|-1) dA' \quad (253)$$

and the additional operator for a perfectly conducting ground plane which is in a form consistent with the actual programming is

$$\frac{\underline{\underline{R}}_z \hat{n}(\underline{r})}{4\pi} \times \int (\underline{\underline{R}}_z \underline{r}-\underline{r}') \times \underline{\underline{I}} \frac{e^{ik|\underline{\underline{R}}_z \underline{r}-\underline{r}'|}}{|\underline{\underline{R}}_z \underline{r}-\underline{r}'|^3} (ik|\underline{\underline{R}}_z \underline{r}-\underline{r}'|-1) dA' \quad (254)$$

where by $\underline{\underline{R}}_z \alpha$ is meant the reflection of α about the ground plane. As can be seen, the two operators have the same form with respect to the variable of integration, \underline{r}' , thus permitting the use of the same subroutines for computing both integrals.

The lossy half-space correction term, however, cannot be cast in this form; hence, separate subroutines are needed. The lossy half-space operator is

$$\hat{n}(\underline{r}) \times \int \left[K_{s\phi z} \hat{a}_{\phi_D} \hat{a}_z + K_{sz\phi} \hat{a}_z \hat{a}_{\phi_D} + K_{s\rho\phi} \hat{a}_{\phi_D} \hat{a}_{\rho_D} + K_{s\rho\phi} \hat{a}_{\rho_D} \hat{a}_{\phi_D} \right] dA' \quad (255)$$

where $K_{s\phi z}$, $K_{sz\phi}$, $K_{s\rho\phi}$ and $K_{s\phi\rho}$ are given by Equations 106-109,

\hat{a}_z is the unit vector perpendicular to the ground plane,
 \hat{a}_{ρ_D} is the direction of the projection onto the ground plane
of the vector from r' to r (if the projection has a zero
length, any given unit vector perpendicular to \hat{a}_z will do),
and $\hat{a}_{\phi_D} = \hat{a}_z \times \hat{a}_{\rho_D}$.

Fortunately, the perfectly conducting operator (and
therefore the free-space operator) can be cast in the same
form as the lossy half-space. For the perfectly conducting
operator,

$$K_{sz\phi} = K_{s\phi z} = \frac{-e^{ik_0 |\underline{R}_z \underline{r} - \underline{r}'|} (ik_0 |\underline{R}_z \underline{r} - \underline{r}'| - 1) \rho_D}{4\pi |\underline{R}_z \underline{r} - \underline{r}'|^3} \quad (256)$$

and

$$K_{s\phi\rho} = -K_{s\rho\phi} = \frac{-e^{ik_0 |\underline{R}_z \underline{r} - \underline{r}'|} (ik_0 |\underline{R}_z \underline{r} - \underline{r}'| - 1)(z+z')}{4\pi |\underline{R}_z \underline{r} - \underline{r}'|^3} \quad (257)$$

By defining the scalar quantities so as to match the perfectly
conducting operator, we were able to test the subroutines that
were written to incorporate the lossy half-space terms. These
subroutines produce the same results as the subroutines that
calculate the perfectly conducting operator.

4. FREE-SPACE LIMIT

As discussed in the preceding subsection, the total
operator is written as the sum of three operators. For the

special case of the half-space having dielectric properties similar to those of free-space, the total operator should be similar to that of the free-space operator; i.e., the second and third operators should have similar magnitudes but opposite signs. Having verified that the code had this property, we exhausted the available checks on the incorporation of the new terms.

5. COMPARISON TO ANOTHER CODE

G. J. Burke of Lawrence Livermore Laboratory provided us with predictions by the NEC-(1,2)A code of the bulk current induced on a cylinder in the vicinity of a lossy half-space. The parameters of the case are shown in Table 1. The results of the two codes are shown in Table 2. Our results were obtained by a four-point averaging of the longitudinal current densities at a given distance from the center of the cylinder. The discrepancy between the two predictions, less than 5 percent, can be attributed to the large zone sizes used by both codes, although certain differences in the modelling assumptions could also contribute to this small error.

6. COMPARISON TO EXPERIMENTAL DATA

Here we present comparisons of our code's surface current predictions to experimental data obtained at the University of Michigan. The first three figures (Figures 5-7) are reproduced from Reference 1; they are included as indications that the experimental equipment is measuring the quantity being predicted by our code. The remaining three figures (Figures 8-10) show how the experimental data for a cylinder above a lossy planar surface compares to our predictions of surface current for a cylinder above a half-space having the same dielectric properties as the planar surface. Table 3 describes these dielectric properties. For each graph, the solid curves are subjectively smoothed traces, i.e., spikes

TABLE 1. CONFIGURATION PARAMETERS
FOR COMPARISON TO THE
LAWRENCE LIVERMORE
LABORATORY'S NUCLEAR
ELECTROMAGNETICS CODE
(L³NEC)

Wavelength = 1 m
Cylinder radius = 0.025 m
Cylinder length = 0.5 m
Cylinder height above half-space = 0.1 m
Relative dielectric constant = 8 + i8

TABLE 2. PREDICTED BULK CURRENTS

Distance from midpoint of cylinder (m)	MFIE	L ³ NEC	Percent difference
0.0	0.00395	0.00413	4.6
0.0714	0.00370	0.00380	2.7
0.1429	0.00289	0.00287	0.7
0.2143	0.00151	0.00144	4.6

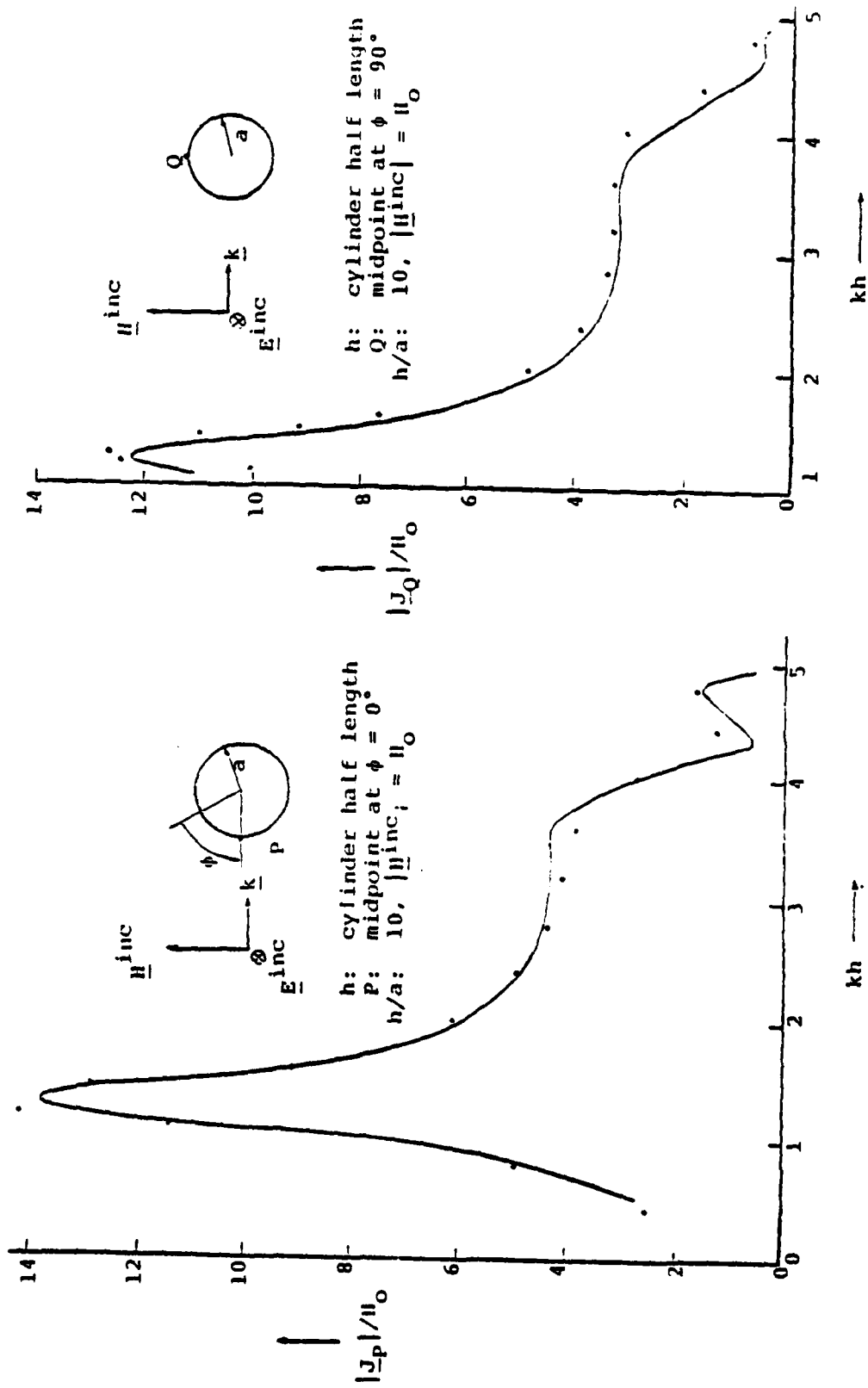


Figure 5. Comparison between "Free Cylinder" experimental results at University of Michigan (solid curves) and MFIE computer code (dots).

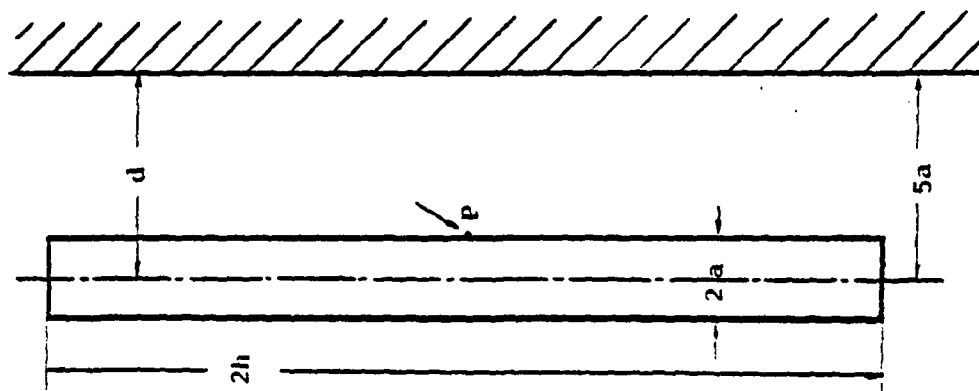
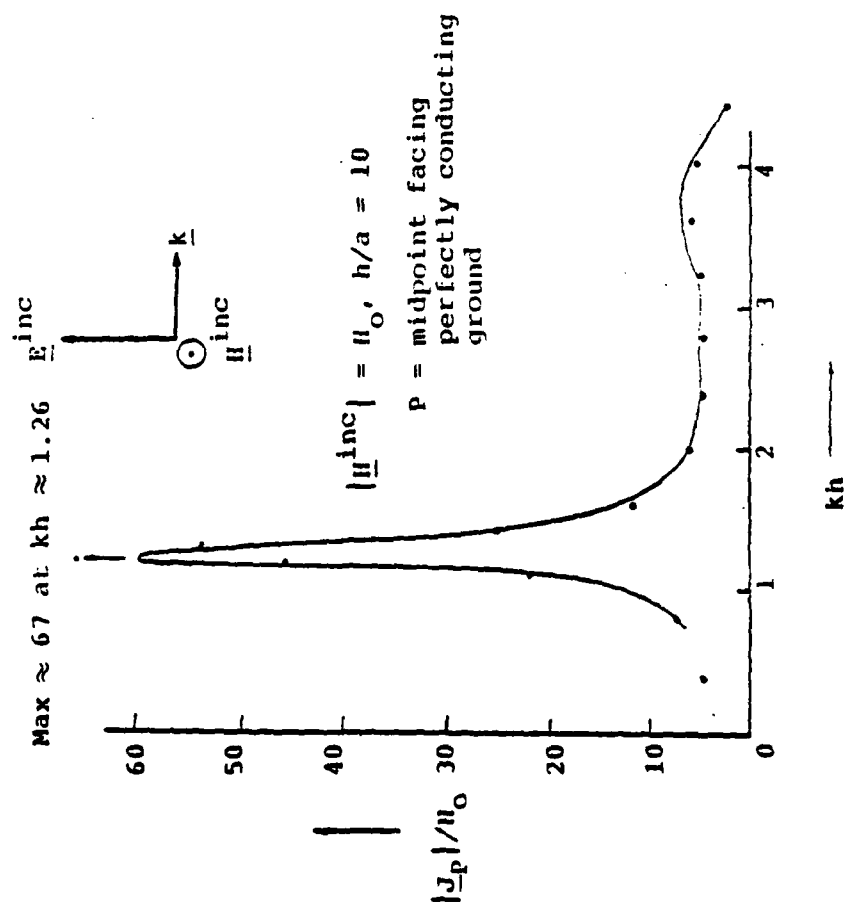


Figure 6. Comparison between "Cylinder Parallel to a Perfectly Conducting Ground" experimental results at University of Michigan (solid curve) and MFIE computer code (dots) for $d = 5a$.

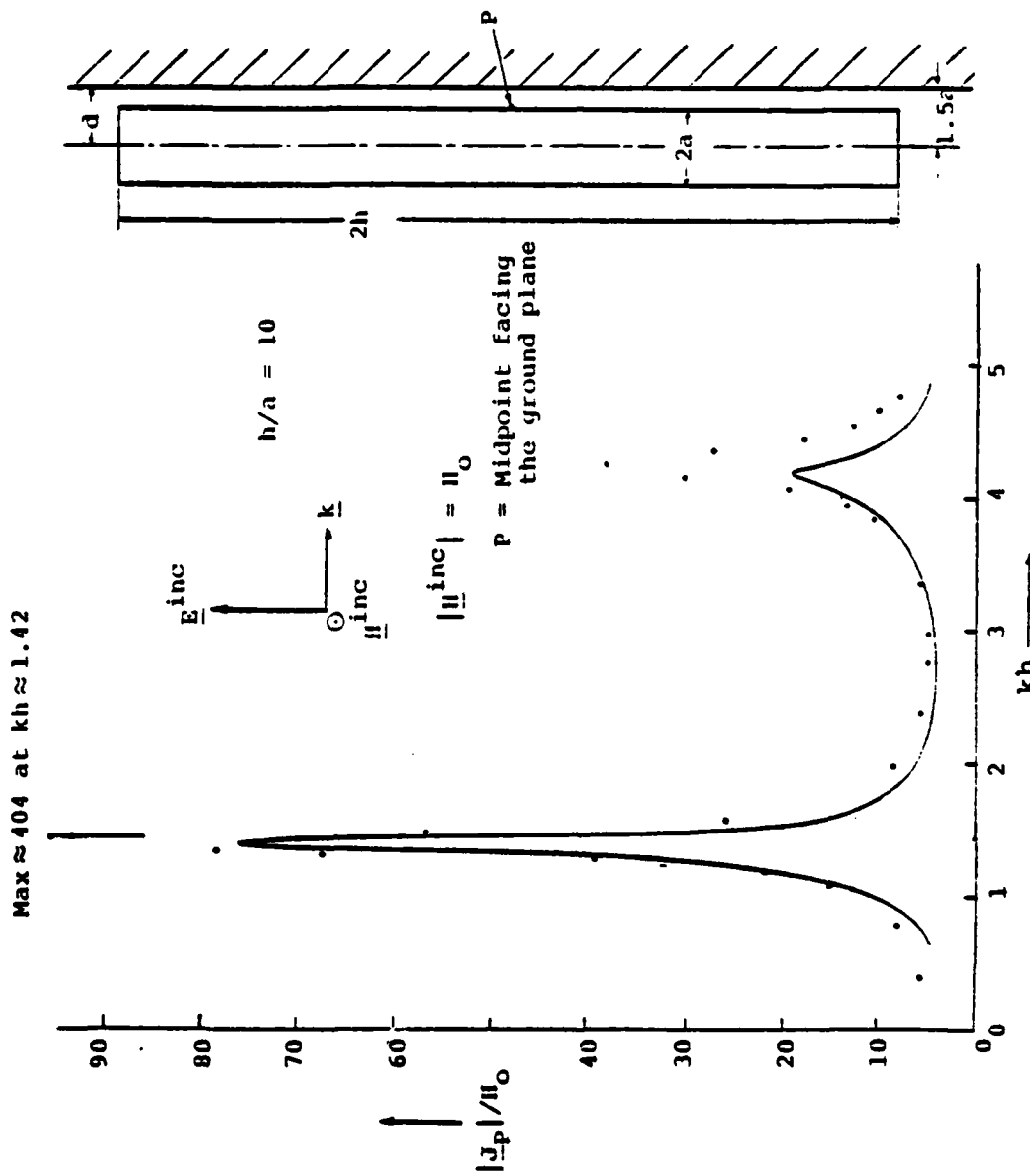


Figure 7. Comparison between "Cylinder Parallel to Perfectly Conducting Ground" experimental results at University of Michigan (solid curve) and MFIE computer code (dots) for $d = 1.5a$.

TABLE 3. COMPLEX DIELECTRIC CONSTANT USED IN
THE MFIE COMPUTER CODE CALCULATIONS
APPLICABLE FOR THE UNIVERSITY OF
MICHIGAN EXPERIMENTAL DATA

Actual frequency of experiment (GHz)	kh used in the code	ϵ_{2R}/ϵ_0	ϵ_{2I}/ϵ_0
0.61	0.7	11.7	15.6
0.78	0.9	10.4	13.2
0.87	1.0	9.6	12.5
0.95	1.1	9.0	12.0
1.00	1.15	8.7	11.6
1.04	1.2	8.6	11.2
1.09	1.25	8.5	11.0
1.13	1.3	8.1	10.6
1.17	1.35	7.9	10.4
1.22	1.4	7.8	10.2
1.30	1.5	7.3	10.0
1.48	1.7	6.8	9.3
1.74	2.0	6.3	8.2
2.08	2.4	5.7	7.9
2.43	2.8	4.6	7.3
2.78	3.2	4.3	6.5
3.13	3.6	4.2	6.0
3.47	4.0	4.0	5.4

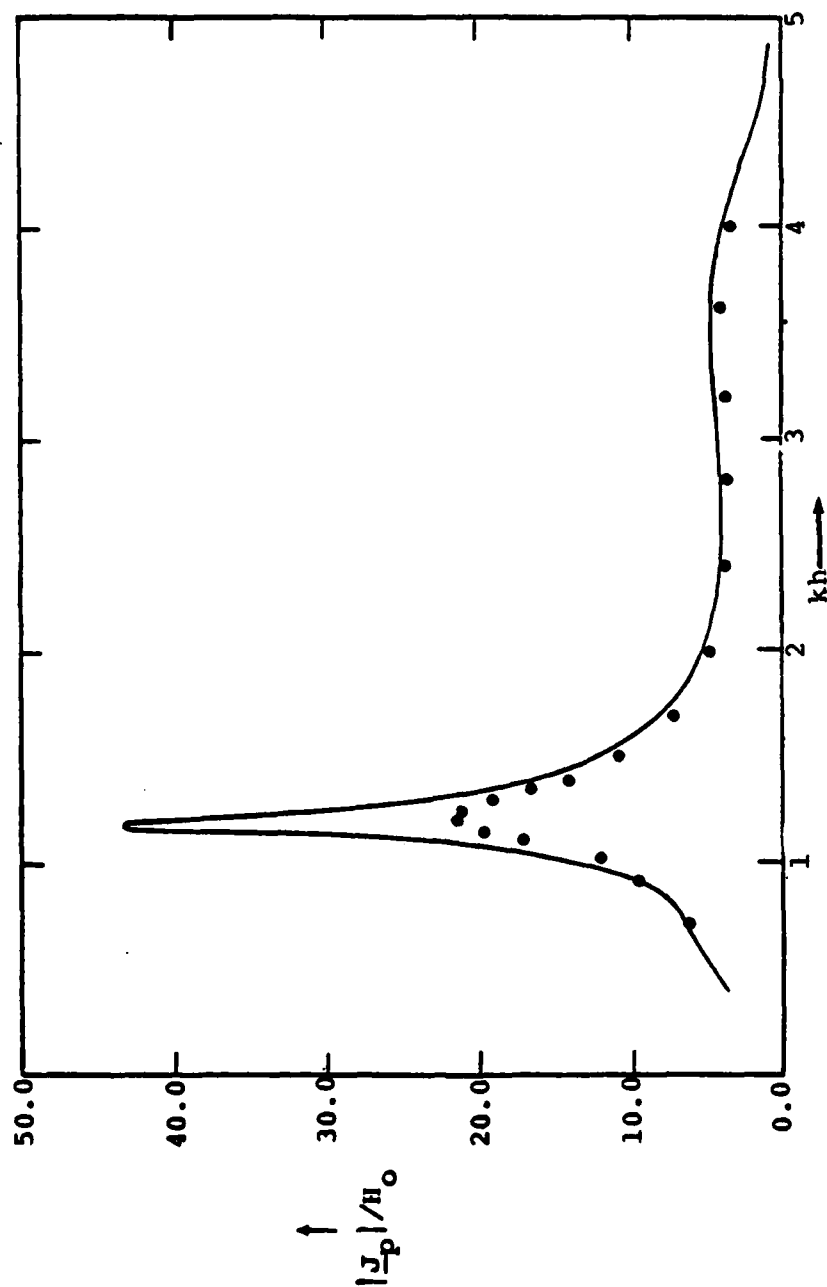


Figure 8. Comparison between the MFIE computer code (dots) and the cylinder parallel to a finitely conducting ground experimental results at University of Michigan (solid curve) for $d = 5a$.

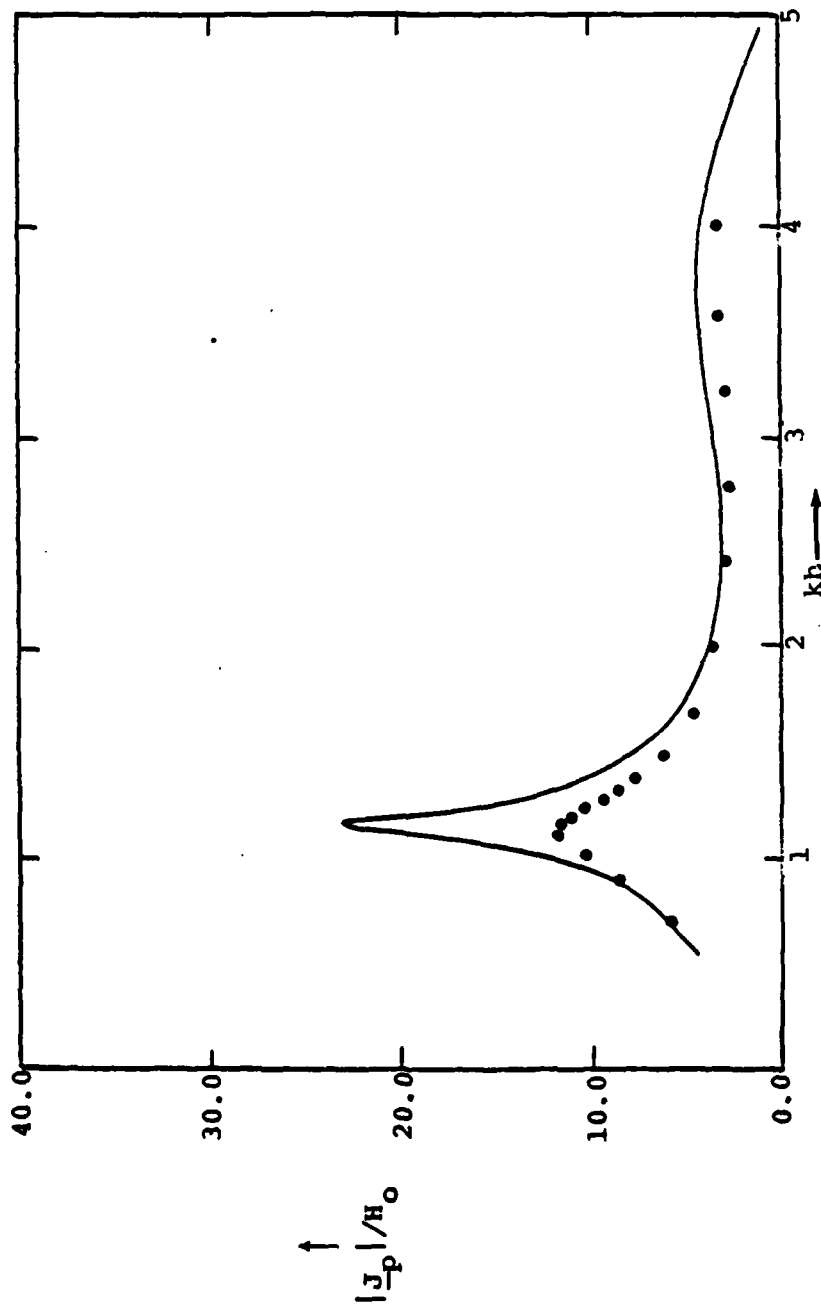


Figure 9. Comparison between the MFIE computer code (dots) and the cylinder parallel to a finitely conducting ground experimental results at University of Michigan (solid curve) for $d = 2a$.

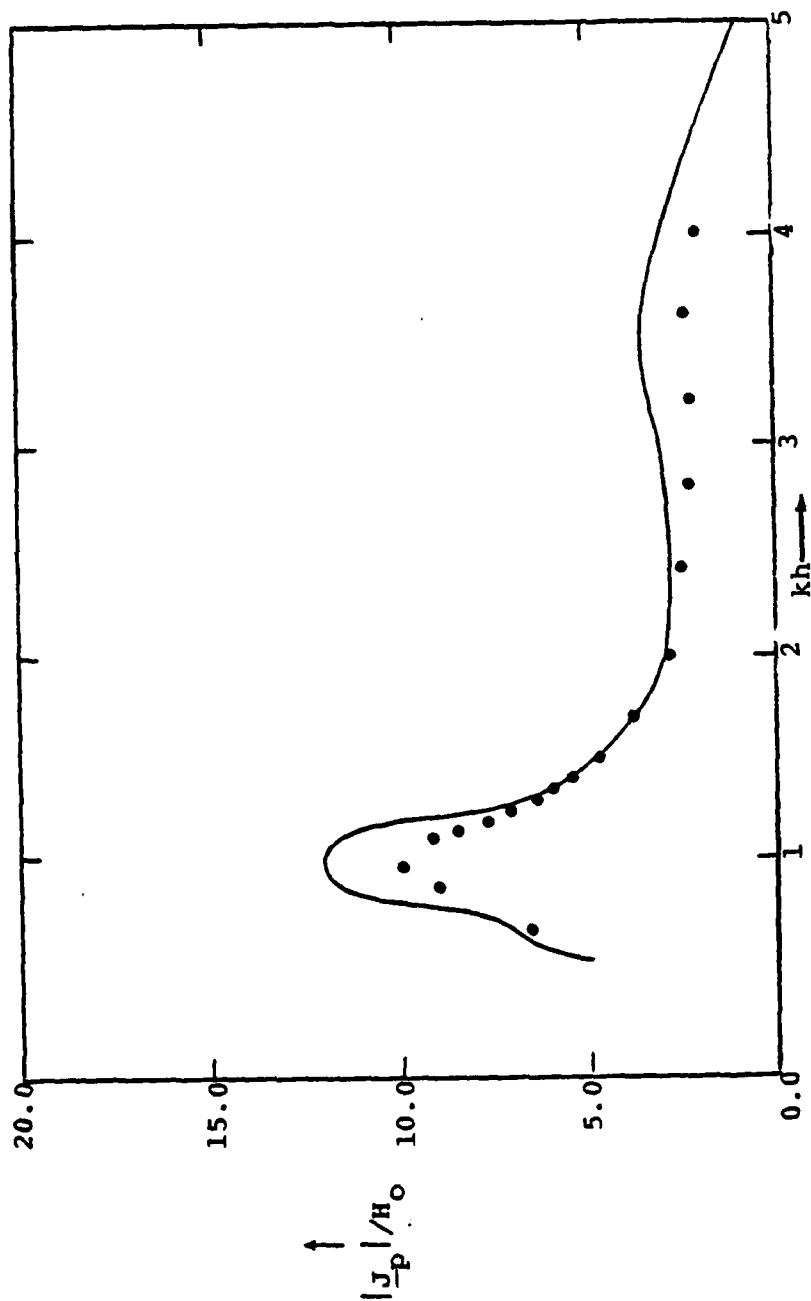


Figure 10. Comparison between the MFIE computer code (dots) and the cylinder parallel to a finitely conducting ground experimental results at University of Michigan (solid curve) for $d = 1.5a$.

eliminated, of experimental data while the dots are the values predicted by our code; see Reference 1 for the original experimental curves.

We observe that except at resonance the agreement between prediction and experiment is excellent for the free-space case and the case of a cylinder above a perfectly conducting ground plane. The fact that the agreement suffered most at resonance is not surprising since this region is most sensitive to detailed modelling accuracy.

The same cylinder, source and probe were used to measure the cylinder's response to the incident wave in the free-space, perfectly conducting half-space, and lossy half-space configurations. Therefore, we will use the level of agreement obtained for the two former configurations as a basis for comparing the predictions to the experimental data for the lossy material. According to this criterion, although there is general qualitative agreement, the quantitative agreement suffers by comparison to the earlier efforts.

This disagreement does not necessarily invalidate either the experiment or the computer code. An alternative is the possibility that the differences between the experimental configuration and the configuration being modelled by the code are significant. Take, for example, the lossy ground plane used in the experiment. It consisted of 12 slabs assembled into three layers 4 ft x 4 ft x 2½ in. supported by a metallic ground plane. How this compares to a half-space is in question. (Of course, if we believe both the experimental and predictive results, the question is answered.)

7. ACCURACY CONSIDERATIONS

The MFIE is a direct consequence of Maxwell's equations for the problem being solved: electromagnetic scattering from a perfect conductor embedded inside a layer of a stratified

medium. However, the numerical approximation used for solving this equation, patch zoning, cannot be performed with complete precision in a finite time. Besides the approximation inherent in the technique (piecewise constant solutions), the matrix elements must be approximated since the kernels of the associated integrals cannot be integrated in closed form; in fact, for the lossy half-space terms, the kernels are themselves integrals which cannot be integrated in closed form.

The parameters affecting solution accuracy are:

1. Zoning density
2. Quadrature order for spatial integration
3. Accuracy of the terms due to the lossy half-space

The first item has been programmed as input variables; the user of the program decides their values. Our choice for the second and third parameters was dictated by the joint criteria of minimizing computation time and restricting the induced error in the solution to less than ten percent.

The scheme used for the spatial integration was:

1. For the free-space term, and therefore the perfectly conducting term, reduce the two-dimensional integral to a one-dimensional integral of a finite sum of terms. This step removes the difficulty of performing numerical integration on a singular integral without introducing an error which is large compared to machine roundoff.
2. The remaining integration was performed using two-point Gaussian quadrature.
3. The lossy half-space terms were integrated by a product rule of Gaussian quadrature, i.e., a three-point rule for one direction of integration and a two-point rule for the other direction.

The final consideration was the generation of the lossy half-space terms. Their generation by numerical integration proved to be prohibitively expensive thus forcing us to develop an interpolation scheme for these terms. We found that even in severe tests of our scheme, a 30 by 30 interpolation table proved sufficient to obtain the same final answer, to within one percent, as the same case using direct calculation of these terms.

REFERENCES

1. Sancer, M. I., Siegel, S., and Varvatsis, A. D., Formulation of Electromagnetic Pulse External Interaction Above a Lossy Earth/Comparison of Numerical Results with Experimental Data for Limiting Cases, TDR, Inc., AFWL Interaction Note 354, October, 1978.
2. Felsen, L. B., and Marcuvitz, N., Radiation and Scattering of Waves, Prentice-Hall, Englewood Cliffs, N.J., 1973.
3. Baños, A., Dipole Radiation in the Presence of a Conducting Half-Space, Pergamon Press, Oxford, 1966.
4. Haddad, H. A., and Chang, D. C., Dyadic Green's Function for a Two-Layered Earth, University of Colorado, AFWL Mathematics Note 50, February, 1977.
5. Wait, J. R., Electromagnetic Waves in Stratified Media, The MacMillan Company, New York, 1962.
6. Liepa, V. V., Sengupta, D. L., Ferris, J. E., and Senior, T.B.A., Surface Field Measurements with Image and Ground Planes, University of Michigan, AFWL Sensor and Simulation Note 244, November, 1977.
7. Burke, G. J., and Poggio, A. J., Numerical Electromagnetic Code (NEC) Method of Moments Volume I - Program Description Theory, Lawrence Livermore Laboratory, AFWL Interaction Note 363, July, 1977.
8. Lee, K.S.H., Marin, L., and Castillo, J. P., Limitations of Wire-Grid Modeling of a Closed Surface, the Dikewood Corporation/Air Force Weapons Laboratory, AFWL Interaction Note 231, May, 1975.
9. Kuo, W. C., and Mei, K. K., "Numerical Approximations of the Sommerfield Integral for Fast Convergence", Radio Science, Vol. 13, No. 3, May-June 1978, p. 407.

APPENDIX A. PROOF THAT $F_{N_s ab}$ IS INDEPENDENT
OF THE SCATTERING OBJECT

For convenience we begin our proof by defining the quantity

$$A_\ell = I_{s\ell, \ell-1} + I_{s\ell, \ell+1} \quad \ell=2, \dots, N-1 \quad (A-1)$$

where $I_{s\ell, k}$ is defined in Equation 10. The definitions for $\ell = 1$ and $\ell = N$ require further explanation. For $\ell = N$, $I_{sN, N+1}$ equals the limit of the integral over a hemispherical surface having a radius approaching infinity. Because of the radiation condition (or exponential damping if ϵ_N is lossy) imposed on the fields, this limit is zero. The case $\ell = 1$ is treated differently for the horizontally stratified medium and the radially stratified medium. For the horizontally stratified medium, $I_{s1, 0}$ equals the limit of the integral over a hemispherical surface having a radius approaching infinity; it is zero for the same reason as $I_{sN, N+1}$. For the spherically stratified case, an $I_{s1, 0}$ never really exists. Using this information, we complete the presentations for the A_ℓ 's for both the horizontally stratified and the radially stratified medium situations as follows:

$$A_1 = I_{s1, 2} \quad (A-2)$$

$$A_N = I_{sN, N-1} \quad (A-3)$$

In arriving at the expressions contained in Equations A-2 and A-3, it was necessary to use the boundary conditions at infinity satisfied by the fields. In order to obtain the following relationship which plays an important role in this proof

$$I_{sj,k} = -I_{sk,j} \quad k=j\pm 1 \quad (A-4)$$

it will be necessary to employ the boundary conditions satisfied by the fields at each interface. Combining Equations 8 and 10, we have

$$I_{sj,k} = \int_{S_{j,k}} m_{jk} dS \quad (A-5)$$

where

$$m_{jk} = \hat{n}_{jk} \cdot [\underline{E}_{ja} \times \underline{H}_{jb} - \underline{E}_{jb} \times \underline{H}_{ja}] \quad (A-6)$$

Using the fact that for general vectors \underline{A} and \underline{B} ,

$$\hat{n} \cdot [\underline{A} \times \underline{B}] = \hat{n} \cdot [\underline{A}_t \times \underline{B}_t] \quad (A-7)$$

where

$$\underline{A}_t = \underline{A} \cdot [\underline{I} - \hat{n}\hat{n}] \quad (A-8)$$

we can rewrite Equation A-6 as

$$m_{jk} = \hat{n}_{jk} \cdot [\underline{E}_{tja} \times \underline{H}_{tjb} - \underline{E}_{tjb} \times \underline{H}_{tja}] \quad (A-9)$$

Now the boundary conditions at the S_{jk} interface are such that

$$\underline{E}_{tja} = \underline{E}_{tka} \quad \alpha=a,b \quad (A-10)$$

and

$$\underline{H}_{tj\alpha} = \underline{H}_{tk\alpha} \quad \alpha=a,b \quad (A-11)$$

Using the fact $\hat{n}_{j,k} = -\hat{n}_{k,j}$ together with Equations A-9, A-10, and A-11, it follows that

$$m_{jk} = -m_{kj} \quad (A-12)$$

This, combined with the fact that $S_{j,k}$ and $S_{k,j}$ denote the same interfacing proves Equation A-4. Using Equations A-1 through A-4 and forming the sum

$$S = \sum_{\ell=1}^N A_{\ell} \quad (A-13)$$

we can conclude that $S=0$, or equivalently that

$$A_{N_s} = - \sum_{\substack{\ell=1 \\ \ell \neq N_s}}^N A_{\ell} \quad (A-14)$$

Since $J_{\ell a} \equiv 0$ for $\ell \neq N_s$, the definition of A_{ℓ} in conjunction with Equation 9 implies

$$A_{\ell} = -I_{V\ell ab} \quad \ell \neq N_s \quad (A-15)$$

Rewriting Equation 15, which appeared in Section 2, as

$$F_{N_s ab} = A_{N_s} + I_{VN_s ab} \quad (A-16)$$

and substituting Equations A-14 and A-15 into this equation, we obtain

$$F_{N_s ab} = \sum_{\ell=1}^N I_{V\ell ab} \quad (A-17)$$

In order to draw our desired conclusion, it is only necessary to show that $I_{V\ell ab}$ is independent of the scattering object. To do this, we write the definition of this quantity given by Equation 12 in expanded form as follows:

$$I_{V\ell ab} = \int_{V_{\ell b}} \underline{E}_{\ell}(\underline{r}, \underline{r}_a) \cdot \underline{J}_{\ell b}(\underline{r}) dV \quad (A-18)$$

The quantity $\underline{E}_{\ell}(\underline{r}, \underline{r}_a)$ is the electric field, observed at a point $\underline{r} \in V_{\ell}$, produced by the current distribution; $\underline{J}_{N_s a} = \hat{a} \delta(\underline{r} - \underline{r}_a)$, with the scattering object considered to be absent; and $\underline{J}_{\ell b}$ is a rigid source unaffected by the scattering object. Thus, it follows that $I_{V\ell ab}$ is independent of the scatterer, and from Equation A-17 it follows that $F_{N_s ab}$ is independent of the scatterer.

APPENDIX B. PROOF THAT $\underline{G}_j(\underline{r}, \underline{r}') = \underline{G}_k(\underline{r}', \underline{r})$

The proof is started by taking the curl of Equations 39 and 47 and then substituting Equations 40 and 41 into the results to obtain

$$\nabla \times \underline{G}_\ell(\underline{r}, \underline{r}') = i\omega\mu_\ell \underline{K}_\ell(\underline{r}, \underline{r}') \quad (B-1)$$

$$\nabla \times \underline{K}_\ell(\underline{r}, \underline{r}') = -i\omega\epsilon_\ell \underline{G}_\ell(\underline{r}, \underline{r}') + \delta(\underline{r} - \underline{r}') \sum_{i=1}^3 \hat{a}_i \hat{a}_i$$

$$= -i\omega\epsilon_\ell \underline{G}_\ell(\underline{r}, \underline{r}') + \delta(\underline{r} - \underline{r}') \underline{I} \quad (B-2)$$

We now consider the special cases in which the source point \underline{r}' is restricted to lie in the volumes V_j or V_k , and we introduce the notation

$$\underline{r}' = \underline{r}_a \in V_j \quad (B-3)$$

$$\underline{r}' = \underline{r}_b \in V_k \quad (B-4)$$

Next we take the dot product from the right with the vector \underline{a}

$$\underline{a} = \underline{a} \quad \ell=j \quad (B-5)$$

$$\underline{a} = \underline{b} \quad \ell=k \quad (B-6)$$

with both sides of Equations B-1 and B-2 to obtain Equations 1 and 2 after making the identifications

$$\underline{G}_\ell(\underline{r}, \underline{r}_\alpha) \cdot \underline{\alpha} = \underline{E}_\ell(\underline{r}, \underline{r}_\alpha) \quad (\text{B-7})$$

$$\underline{K}_\ell(\underline{r}, \underline{r}_\alpha) \cdot \underline{\alpha} = \underline{H}_\ell(\underline{r}, \underline{r}_\alpha) \quad (\text{B-8})$$

$$\underline{J}_{\ell\alpha}(\underline{r}) = \underline{\alpha} \delta(\underline{r} - \underline{r}_\alpha) \quad (\text{B-9})$$

It now follows that Equations 9 through 12 are valid for the quantities just defined. Noting that the scattering surface plays no role in the analysis presented in this appendix, we write Equation 9 as

$$A_\ell = I_{V\ell ba} - I_{V\ell ab} \quad (\text{B-10})$$

where we have incorporated the definition for A_ℓ given in Appendix A. Because of our choice of sources, it follows that

$$A_j = I_{Vjba} \quad (\text{B-11})$$

$$A_k = -I_{Vkab} \quad (\text{B-12})$$

$$A_\ell = 0 \quad \ell \neq j, k \quad (\text{B-13})$$

As argued in Appendix A, the boundary conditions guarantee that

$$\sum_{\ell=1}^N A_\ell = 0 \quad (\text{B-14})$$

Combining Equations B-9 through B-12, it follows

$$I_{Vjba} = I_{Vkab} \quad (B-15)$$

Using Equations 5 and 12 as well as Equations B-5 through B-9 to represent Equation B-15 in more detail, and evaluating the volume integrals using the properties of the δ function, we obtain

$$\underline{a} \cdot \underline{G}_j(\underline{r}_a, \underline{r}_b) \cdot \underline{b} = \underline{b} \cdot \underline{G}_k(\underline{r}_b, \underline{r}_a) \cdot \underline{a} \quad (B-16)$$

Using general properties of the vector dyadic product, we can write

$$\underline{a} \cdot \underline{G}_j(\underline{r}_a, \underline{r}_b) \cdot \underline{b} = \underline{a} \cdot \underline{G}_k^T(\underline{r}_b, \underline{r}_a) \cdot \underline{b} \quad (B-17)$$

Using the fact that \underline{a} and \underline{b} were arbitrarily chosen vectors and changing notation so that $\underline{r}_a = \underline{r}$ and $\underline{r}_b = \underline{r}'$, we obtain the desired result

$$\underline{G}_j(\underline{r}, \underline{r}') = \underline{G}_k^T(\underline{r}', \underline{r}) \quad \underline{r} \in V_j \quad \underline{r}' \in V_k \quad (B-18)$$

APPENDIX C. OUTLINE OF ESSENTIAL DETAILS TO DERIVE EQUATION 38

An essential difference in obtaining Equation 38 as opposed to Equation 37, which was derived in detail in Section 2, is the choice of the source $\underline{J}_{\ell a}$. In order to derive Equation 38, we choose

$$\underline{J}_{ka}^i = \hat{a}_i \delta(\underline{r} - \underline{r}_a) \quad i=1,2,3 \quad (C-1)$$

with $\underline{r}_a \in V_{k, k \neq N_s}$, as opposed to the choice expressed by Equation 16. The rigid sources, $\underline{J}_{\ell b}$, are the same physical sources for the excitation as before. We now write Equation 9 as

$$A_k = I_{vkba} - I_{vkab} \quad (C-2)$$

$$A_{N_s} = -I_{VN_s ab} - I_s \quad (C-3)$$

$$A_\ell = -I_{V\ell ab} \quad \ell=1,2,\dots,N \quad \ell \neq k, N_s \quad (C-4)$$

with the meaning of the A_j 's defined in Appendix A. As seen in that appendix

$$\sum_{j=1}^N A_j = 0 \quad (C-5)$$

independent of our choice of sources $\underline{J}_{\ell a}$ and $\underline{J}_{\ell b}$. Combining Equations C-2, C-3, C-4, and C-5 we obtain

$$I_{Vkba} - I_s - \sum_{j=1}^N I_{Vjab} = 0 \quad (C-6)$$

To further interpret this equation, we note that

$$I_{Vkba} = \hat{a} \cdot \underline{E}_{kb}(\underline{r}_a) \quad (C-7)$$

and as in Section 2, \hat{a} can be sequentially chosen as \hat{a}_1, \hat{a}_2 , and \hat{a}_3 . We can now rewrite Equation C-6 as

$$F_{kab} + I_s = \hat{a} \cdot \underline{E}_{kb}(\underline{r}_a) \quad (C-8)$$

$$F_{kab} = \sum_{j=1}^N I_{Vjab} \quad (C-9)$$

and Equation C-8 can be related to Equation 14. In fact, using the evaluation of $F_{N_s ab}$ found in Appendix A and comparing that expression to the expression given for F_{kab} given by Equation C-9, one might conclude that the left-hand side of Equation C-8 is identical to the left-hand side of Equation 14. This is not quite the case because the implicit dependence on \underline{r}_a causes the essential difference. In Equation 14, $\underline{r}_a \in V_{N_s}$, while in Equation C-8, $\underline{r}_a \in V_k$. Despite this difference, the same arguments that were used in Section 2 to arrive at Equation 31 from Equation 14 can be used to arrive at

$$\underline{E}_{kb}(\underline{r}_a) = \underline{E}_{Tkb}(\underline{r}_a) + \int_S \underline{J}(\underline{r}) \cdot \underline{G}_{N_s}(\underline{r}, \underline{r}_a) dS$$

$$\underline{r}_a \in V_k \quad (C-10)$$

when they are applied to Equation C-8. Using Equation B-15, we can write Equation C-10 as

$$\underline{E}_{kb}(\underline{r}_a) = \underline{E}_{Tkb}(\underline{r}_a) + \int_S \underline{G}_k(\underline{r}_a, \underline{r}) \cdot \underline{J}(\underline{r}) dS \quad (C-11)$$

Recognizing that k is a dummy index, which for completeness we now call ℓ , and making the same notation change that was used in Section 2 to arrive at Equation 37 from Equation 36, we can now write Equation C-11 as

$$\underline{E}_{\ell}(\underline{r}) = \underline{E}_{T\ell}(\underline{r}) + \int_S \underline{G}_{\ell}(\underline{r}, \underline{r}') \cdot \underline{J}(\underline{r}') dS' \quad (C-12)$$

which is Equation 38, and thus completes this appendix.